6
Symmetry Aspects and Selection Rules: Group Theory

Symmetry is an important concept in physics. Momentum (angular momentum) conservation, for example, goes hand in hand with the translational (rotational) symmetry of space, and in a periodic lattice, the same can be said for crystal momentum for an electron or phonon state. Many optical processes are governed by conserved physical variables or selection rules that are the consequence of symmetry requirements. The selection rules governing the Raman scattering are derived from group theory which is the central focus of this chapter.

Group theory is a branch of mathematics whose beauty and strength, when applied to physics, resides in the transformation of many complex symmetry operations into a very simple linear algebra. A deep understanding of group theory requires a devoted study [94] and cannot be gained on the basis of this chapter. However, we can in this chapter provide a taste of the basic concepts, the power and usage of group theory in the field of Raman spectroscopy, giving examples of the useful information which comes from its application to the Raman spectroscopy of sp^2 nanocarbons. Therefore, be aware that this chapter may be difficult for a reader without a background in group theory, but with the help of a knowledgeable mentor, the beauty of symmetry can be introduced.

First, in Section 6.1, we briefly present the basic concepts of group theory [94] as they are applied to Raman spectroscopy. In Section 6.2 we give a group theoretical treatment of the Raman scattering selection rules. Section 6.3 summarizes a group theory analysis of optical processes for electrons and phonons in monolayer, bilayer and trilayer graphene, and extending all the way to N layer graphene, distinguishing the cases of even N, odd N and very large N, the latter corresponding to graphite [98, 217]. The symmetry of graphene is chosen for the introduction to this topic because the graphene family provides the fundamental building blocks for all sp^2 carbons, and monolayer graphene (1-LG) is the building block for all graphenes. In the second half of the chapter, we summarize in Section 6.4 the symmetry properties of single-wall carbon nanotubes (SWNTs) [135, 218], including an interesting connection given in Section 6.4.6 between the nature of the selection rules for the scattering processes in one dimension and those pertinent to the unfolded two-dimensional wave vector space [110].

Raman Spectroscopy in Graphene Related Systems. Ado Jorio, Riichiro Saito, Gene Dresselhaus, and Mildred S. Dresselhaus

ISBN: 978-3-527-40811-5

6.1
The Basic Concepts of Group Theory

6.1.1
Definition of a Group

The structure of sp^2 nanocarbons can be constructed by considering one single C atom and applying successively all the symmetry operations that take one atom into another, which include rotations, reflections, inversion, translations and combined operations. The set of symmetry operations that a molecule or crystal exhibits form a group in the group theory sense, and a group is defined as the following. A collection of elements $A, B, C, \ldots$ form a group when the following four conditions are satisfied:

1. The product of any two elements of the group is itself an element of the group. For example, relations of the type $AB = C$ are valid for all members of the group.
2. The associative law is valid, that is, $(AB)C = A(BC)$.
3. There exists a unit element E (also called the identity element) such that the product of E with any group element leaves that element unchanged $AE = EA = A$.
4. For every element A there exists an inverse element A^{-1} such that $A^{-1}A = AA^{-1} = E$.

As a simple example of a group, consider the permutation group for three numbers, $P(3)$. Below are listed the $3! = 6$ possible permutations that can be carried out; the top row denotes the initial arrangement of the three numbers and the bottom row denotes the final arrangement. Each permutation is an element of $P(3)$.

$$E = \begin{pmatrix} 1 & 2 & 3 \\ 1 & 2 & 3 \end{pmatrix} \quad A = \begin{pmatrix} 1 & 2 & 3 \\ 1 & 3 & 2 \end{pmatrix} \quad B = \begin{pmatrix} 1 & 2 & 3 \\ 3 & 2 & 1 \end{pmatrix}$$
$$C = \begin{pmatrix} 1 & 2 & 3 \\ 2 & 1 & 3 \end{pmatrix} \quad D = \begin{pmatrix} 1 & 2 & 3 \\ 3 & 1 & 2 \end{pmatrix} \quad F = \begin{pmatrix} 1 & 2 & 3 \\ 2 & 3 & 1 \end{pmatrix}. \tag{6.1}$$

We can also think of the elements in Eq. (6.1) in terms of the three points of an equilateral triangle (see Figure 6.1). Again, the top row denotes the initial state and the bottom row denotes the final position of each number as the effect of the six distinct symmetry operations that can be performed on these three points (see caption to Figure 6.1). The element D is a clockwise rotation of $2\pi/3$ and F is a counter-clockwise rotation of $2\pi/3$. We can call each symmetry operation an *element* of the group. This group is, therefore, identical with the group $P(3)$.

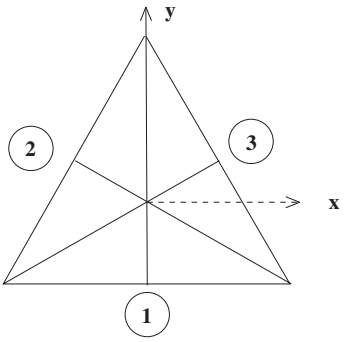

Figure 6.1 The symmetry operations on an equilateral triangle, are the rotations by $\pm 2\pi/3$ about the origin 0 and the rotations by 180° (π) about the three two-fold axes. Here the three two-fold axes are denoted by numbers in circles.

We illustrate the use of the notation by verifying the *associative law* $(AB)C = A(BC)$ for a few elements:

$$\begin{aligned} (AB)C &= DC = B \\ A(BC) &= AD = B\,. \end{aligned} \tag{6.2}$$

Point groups are groups without translations. There is at least one point which does not move under all the operations of a point group. The groups where translations are included as elements are named space groups.

6.1.2 Representations

Two groups are *isomorphic* or *homomorphic* if there exists a correspondence between their elements, such that $A \to \mathcal{A}$, $B \to \mathcal{B}$ and $AB \to \mathcal{AB}$, where the plain letters denote elements in one group and the other letters denote elements in the second group. If the two groups have the same order (same number of elements, such as $P(3)$ and the symmetries of an equilateral triangle), then they are *isomorphic* (one-to-one correspondence). Otherwise they are *homomorphic* (many-to-one correspondence).

The *representation*[1] for an element R (e. g., $R = A, B, C, \ldots$) denoted by $D(R)$ is given by a square matrix in which a set of basis functions $\boldsymbol{u} \equiv (u_1, u_2, \cdots, u_m)$ are transformed by R as

$$R\boldsymbol{u} = D(R)\boldsymbol{u}\,. \tag{6.3}$$

In this way we assign a matrix $D(A)$ to each element A of the group such that $D(RR') = D(R)D(R')$.

1) The representation of an abstract group is a substitution group (matrix group with square matrices) such that the substitution group is homomorphic (or isomorphic) to the abstract group.

Consider the following group of matrices:

$$E = \begin{pmatrix} 1 & 0 \\ 0 & 1 \end{pmatrix} \quad A = \begin{pmatrix} -1 & 0 \\ 0 & 1 \end{pmatrix} \quad B = \begin{pmatrix} \frac{1}{2} & -\frac{\sqrt{3}}{2} \\ -\frac{\sqrt{3}}{2} & -\frac{1}{2} \end{pmatrix}$$
$$C = \begin{pmatrix} \frac{1}{2} & \frac{\sqrt{3}}{2} \\ \frac{\sqrt{3}}{2} & -\frac{1}{2} \end{pmatrix} \quad D = \begin{pmatrix} -\frac{1}{2} & \frac{\sqrt{3}}{2} \\ -\frac{\sqrt{3}}{2} & -\frac{1}{2} \end{pmatrix} \quad F = \begin{pmatrix} -\frac{1}{2} & -\frac{\sqrt{3}}{2} \\ \frac{\sqrt{3}}{2} & -\frac{1}{2} \end{pmatrix}. \tag{6.4}$$

The matrix corresponding to the identity operation is always a unit matrix. The matrices in Eq. (6.4) constitute a matrix representation of the group that is isomorphic to $P(3)$ and to the symmetry operations on an equilateral triangle, since they obey the same multiplication rules. The A matrix represents a rotation by $\pm\pi$ about the y axis while the B and C matrices, respectively, represent rotations by $\pm\pi$ about axes 2 and 3 in Figure 6.1. D and F, respectively, represent rotation of $-2\pi/3$ and $+2\pi/3$ around the center of the triangle (see Section 6.1.1).

6.1.3
Irreducible and Reducible Representations

When $D(R)$ for all the elements in a group can be blocked into similar sub-matrices by one unitarity transformation,[2] the $D(A)$ is called a reducible representation. In this case, the space of $\boldsymbol{u}$ can be decomposed into smaller spaces of basis functions with smaller dimensions. If $D(A)$ cannot be reduced any further into smaller blocks, then $D(A)$ is called an *irreducible representation* (IR).

Three irreducible representations for the permutation group $P(3)$ are:

$$\begin{array}{lccc} & E & A & B \\ \Gamma_1: & (1) & (1) & (1) \\ \Gamma_{1'}: & (1) & (-1) & (-1) \\ \Gamma_2: & \begin{pmatrix} 1 & 0 \\ 0 & 1 \end{pmatrix} & \begin{pmatrix} -1 & 0 \\ 0 & 1 \end{pmatrix} & \begin{pmatrix} \frac{1}{2} & -\frac{\sqrt{3}}{2} \\ -\frac{\sqrt{3}}{2} & -\frac{1}{2} \end{pmatrix} \end{array}$$
$$\begin{array}{lccc} & C & D & F \\ \Gamma_1: & (1) & (1) & (1) \\ \Gamma_{1'}: & (-1) & (1) & (1) \\ \Gamma_2: & \begin{pmatrix} \frac{1}{2} & \frac{\sqrt{3}}{2} \\ \frac{\sqrt{3}}{2} & -\frac{1}{2} \end{pmatrix} & \begin{pmatrix} -\frac{1}{2} & \frac{\sqrt{3}}{2} \\ -\frac{\sqrt{3}}{2} & -\frac{1}{2} \end{pmatrix} & \begin{pmatrix} -\frac{1}{2} & -\frac{\sqrt{3}}{2} \\ \frac{\sqrt{3}}{2} & -\frac{1}{2} \end{pmatrix} \end{array}. \tag{6.5}$$

$\Gamma_1, \Gamma_{1'}$ and Γ_2 obey the same multiplication rules as $P(3)$ and as the equilateral triangle. However, Γ_1 and $\Gamma_{1'}$ are one-dimensional representations having only one and two elements, respectively, being homomorphic to $P(3)$ and to the equilateral triangle. The one-dimensional Γ_1 is named the totally symmetric representation and it exists for all groups. The basis function of the irreducible representation

2) A unitary transformation is an operation such as $UD(R)U^{-1}$, where U is an unitary matrix. For space symmetry operations, such transformations are equivalent to a rotation (without deformation) of the coordinate axes.

Γ_1 does not change the form for any of the operations of the group, such as 1 or $r = x^2 + y^2$ for a bidimensional point group using the spacial coordinates. Thus the dimension of Γ_1 is one and the matrix representation is a 1×1 matrix whose matrix element is 1. For $\Gamma_{1'}$, z is a suitable basis function. By considering the equilateral triangle in the xy plane, the z coordinate goes into $-z$ when applying the symmetry operations A, B and C. Thus the dimension of $\Gamma_{1'}$ is one and the matrix representation is a 1×1 matrix whose matrix element now is either 1 or -1. The bidimensional Γ_2 has six elements and is isomorphic to $P(3)$, as stated previously. A suitable set of basis functions (two orthogonal functions are needed) using the spacial coordinates is (x, y). A reducible representation containing these three irreducible representations is:

$$\begin{array}{cccc} & E & A & B \\ \Gamma_R: & \begin{pmatrix} 1 & 0 & 0 & 0 \\ 0 & 1 & 0 & 0 \\ 0 & 0 & 1 & 0 \\ 0 & 0 & 0 & 1 \end{pmatrix} & \begin{pmatrix} 1 & 0 & 0 & 0 \\ 0 & -1 & 0 & 0 \\ 0 & 0 & -1 & 0 \\ 0 & 0 & 0 & 1 \end{pmatrix} & \begin{pmatrix} 1 & 0 & 0 & 0 \\ 0 & -1 & 0 & 0 \\ 0 & 0 & \frac{1}{2} & -\frac{\sqrt{3}}{2} \\ 0 & 0 & -\frac{\sqrt{3}}{2} & -\frac{1}{2} \end{pmatrix} \end{array} \quad \text{, etc.,} \tag{6.6}$$

where Γ_R is of the block form[3]

$$\left(\begin{array}{c|c|c} \Gamma_1 & 0 & \mathcal{O} \\ \hline 0 & \Gamma_{1'} & \mathcal{O} \\ \hline \mathcal{O} & \mathcal{O} & \Gamma_2 \end{array}\right) . \tag{6.7}$$

It is customary to list the irreducible representations (IR) contained in a reducible representation Γ_R as:

$$\Gamma_R = \Gamma_1 + \Gamma_{1'} + \Gamma_2 . \tag{6.8}$$

In quantum mechanics, the matrix representation of a group, $D(R)$, is important for several reasons. First of all, an eigenfunction for a quantum mechanical operator is a basis function of an IR of the group of the system.[4] Thus, without actually calculating the eigenvalue problem, we can know from group theory the form of functions which belong to each IR.[5] Secondly, quantum mechanical operators are usually written in terms of a matrix representation which is generally a reducible representation of the group, and thus by selecting the basis function belonging to the IR, the matrix can be put into block form. Thus matrix algebra becomes much easier to manipulate than the original symmetry operations.

3) $\mathcal{O}$ indicates a null matrix.

4) Any operator of the group of the system, A commutes with the quantum operator $\mathcal{O}$ as $[A, \mathcal{O}] = 0$. This is a requirement of the group. Then the wavefunction of $A\Psi$ has the same eigenvalue O of $\mathcal{O}$ for Ψ ($\mathcal{O}A\Psi = A\mathcal{O}\Psi = OA\Psi$). Thus Ψ is also an eigenfunction of A (if Ψ is not degenerate) in the group and Ψ is the basis function of an IR. This proof is also valid when E is degenerate.

5) This does not mean that group theory solves the eigenvalue problem. Group theory, however, helps solving the eigenvalue problem by reducing the dimensions of the space to be considered.

6.1.4 The Character Table

The *character* of the representation matrix $D(R)$, is the trace $\chi(R)$ of $D(R)$.[6] The table of $\chi(R)$ for all R and for all IRs constitutes a *character table*, schematically represented in Table 6.1 in which $\chi(R)$ for an IR is listed in a row. The first row of the character table is a totally symmetric IR, denoted by Γ_1 (or $A, A_1, A_g \ldots$ depending on the group and notation) in which all $\chi(R) = 1$. This row is present in the character table for all point groups.

A column of Table 6.1 pertains to a *class* which is defined by a set of operations $(R_1, R_2, \cdots, R_c)$ that transform into one another by any operations O_j in the group such as $R_i = O_j^{-1} R O_j$. For example, if three C_2 rotational operators are equivalent to one another, the three C_2 belong to a class of $3C_2$, where 3 denotes the dimension of the class. The characters for operators within a class are the same. Class 1 in Table 6.1 consists of the identity element E and this element is also present in all groups. The characters for Class 1 for an IR is the dimension of the IR since no basis function changes under the operation E and thus the diagonal matrix elements of $D(E)$ are all 1. Notice that in a group the number of IRs is equal to the number of *classes* in the group.

The character table for the permutation group $P(3)$ is shown in Table 6.2.

Table 6.1 Schematics for a group theory character table. The IR denoted by 1 represents the totally symmetric IR, and is always present in all character tables. $\chi^{\mathcal{C}_k}_{\mathrm{IR}j}$ represents the characters for the symmetry operations in class $\mathcal{C}_k$, belonging to the IR j, where $j = 1, 2, 3$. Also N_k is the number of elements in $\mathcal{C}_k$.

Basis functions		$N_1\mathcal{C}_1$	$N_2\mathcal{C}_2$	$N_3\mathcal{C}_3$
Function 1	IR 1	1	1	1
Function 2	IR 2	$\chi^{\mathcal{C}_1}_{IR2}$	$\chi^{\mathcal{C}_2}_{IR2}$	$\chi^{\mathcal{C}_3}_{IR2}$
Function 3	IR 3	$\chi^{\mathcal{C}_1}_{IR3}$	$\chi^{\mathcal{C}_2}_{IR3}$	$\chi^{\mathcal{C}_3}_{IR3}$

Table 6.2 Character table for the permutation group $P(3)$, for the symmetry operations of the equilateral triangle or, more generally, for the so-called group D_3, using the Schoenflies notation [94].

Class →	$\mathcal{C}_1$	$3\mathcal{C}_2$	$2\mathcal{C}_3$
IR ↓	$\chi(E)$	$\chi(A, B, C)$	$\chi(D, F)$
Γ_1	1	1	1
$\Gamma_{1'}$	1	−1	1
Γ_2	2	0	−1

6) The trace of a matrix is the sum of diagonal matrix elements $\chi(R) = \mathrm{Tr}(R) = \sum_i R_{ii}$.

Table 6.3 Classes for group D_3 or equivalently for the permutation group $P(3)$ and for the symmetry operations of the equilateral triangle.

Notation for each class	D_3	Equilateral triangle	$P(3)$
Class 1 E ($N_k = 1$)	$1\mathcal{C}_1$	(Identity class)	(1)(2)(3)
Class 2 A, B, C ($N_k = 3$)	$3\mathcal{C}_2$	(Rotation of π about two-fold axis)	(1)(23)
Class 3 D, F ($N_k = 2$)	$2\mathcal{C}_3$	(Rotation of 120° about three-fold axis)	(123)

This point group is named D_3 (Schoenflies notation) [94]. In Table 6.2 the notation $N_k\mathcal{C}_k$ is used in the character table to label each class $\mathcal{C}_k$, and N_k is the number of elements in $\mathcal{C}_k$. The classes for group D_3 and $P(3)$ are listed in Table 6.3, showing different ways that the classes of a given group are presented.

6.1.5 Products and Orthogonality

When we define the *inner product* of characters for two IRs weighted by the dimension of the class divided by the normalization factor of the dimension of the group, we get the rules for the ortho-normal conditions for IRs, which is generally referred to as the *Wonderful Orthogonality Theorem for Characters*. To illustrate the meaning of the Wonderful Orthogonality Theorem for Characters, consider the character table for the group $D(3)$ shown in Table 6.2 or given in Table 6.4 in its most commonly used form. Let $\Gamma_j = \Gamma_1$ and $\Gamma_{j'} = \Gamma_{1'}$. Then calculate:

$$\sum_k N_k \chi^{(\Gamma_j)}(\mathcal{C}_k)\left[\chi^{(\Gamma_{j'})}(\mathcal{C}_k)\right]^* = \underbrace{(1)(1)(1)}_{\text{class of } E} + \underbrace{(3)(1)(-1)}_{\text{class of } A,B,C} + \underbrace{(2)(1)(1)}_{\text{class of } D,F}$$

$$= 1 - 3 + 2 = 0. \tag{6.9}$$

It can likewise be verified that the Wonderful Orthogonality Theorem works for all possible combinations of Γ_j and $\Gamma_{j'}$ in Table 6.4.

Since an eigenfunction Ψ for an electron (or phonon) state pertains to a given IR, we identify in the character table the set of symmetry operations that Ψ exhibits, thus describing the effect of the symmetry operations on Ψ based on the simple linear algebra of matrices. The dimension of each IR, d, gives the degeneracy of an

Table 6.4 Character table for group D_3 (rhombohedral).

D_3 (32)			E	$2C_3$	$3C_2'$
$x^2 + y^2, z^2$		A_1	1	1	1
	R_z, z	A_2	1	1	−1
(xz, yz) / $(x^2 - y^2, xy)$	(x, y) / (R_x, R_y)	E	2	−1	0

energy level which belongs to the IR. If the system has m IR eigenstates given by group theoretical considerations as below, we expect to have m, d-fold eigenvalues (this means $m \times d$ eigenfunctions). As shown later, for a chiral nanotube, we have five doubly degenerate Raman-active phonon modes for a given IR (named E_1).

6.1.6 Other Basis Functions

For each symmetry group, one can build a character table whose structure is shown in Table 6.1. We remind readers that the basis function can be obtained by considering the representation matrices and vice-versa. In the leftmost column, the corresponding simple basis functions belong to the IR, such as x, y, z for translation, R_x, R_y, R_z for rotation along the x, y, z axes, or quadratic functions xx, yy, zz, xy, yz, zx and so on. An example is given in Table 6.4 for the D_3 group. This information on the basis functions is useful for knowing which IR belongs to the vibration along the x direction, the rotation along the x axis, and the Raman-active modes (see Section 6.2). The known groups such as point groups, space groups, symmetry groups, are all listed in crystallography tables and their character tables can be found in group theory books.

6.1.7 Finding the IRs for Normal Modes Vibrations

To find the normal modes for the vibration problem, we carry out the following steps:

1. Identify the symmetry operations that define the point group G of the crystal unit cell in its equilibrium configuration.
2. Find the characters for the equivalence representation, $\Gamma_{\text{equivalence}} = \Gamma^{\text{a.s.}}$ (a.s. stands for atom sites). These characters represent the number of atoms that are invariant under the symmetry operations of the group. Since $\Gamma^{\text{a.s.}}$ is, in general, a reducible representation of the group G, we must decompose $\Gamma^{\text{a.s.}}$ into its irreducible representations (e. g., see Eq. (6.8)).
3. We next use the concept that a molecular vibration involves the transformation properties of a vector. In group theoretical terms, this means that the molecular vibrations are found by taking the direct product of $\Gamma^{\text{a.s.}}$ with the irreducible representations for a radial vector (such as (x, y, z)). The representation for the molecular vibrations $\Gamma_{\text{lat. mode}}$ is thus found according to the relation[7)]

$$\Gamma_{\text{lat. mode}} = (\Gamma^{\text{a.s.}} \otimes \Gamma_{\text{vec}}) \, . \tag{6.10}$$

7) If working with molecules, Γ_{trans} and Γ_{rot} have to be subtracted from Eq. (6.10), where Γ_{trans} and Γ_{rot} denote the representations for the simple translations and rotations of the molecule about its center of mass.

The symbol $\otimes$ denotes the direct product of two IRs.[8] The characters found from Eq. (6.10), in general, correspond to a reducible representation of Group G. We therefore express $\Gamma_{\text{lat. mode}}$ in terms of the *irreducible* representations of group G to obtain the normal modes. Each eigenmode is labeled by one of these irreducible representations, and the degeneracy of each eigenfrequency is the dimensionality of the corresponding irreducible representation. The characters for Γ_{trans} are found by identifying the irreducible representations of the group G corresponding to the basis functions (x, y, z) for the radial vector $\boldsymbol{r}$. The characters for Γ_{rot} are found by identifying the irreducible representations corresponding to the basis functions (R_x, R_y, R_z) for the axial vector (e. g., angular momentum which, for example, corresponds to $\boldsymbol{r} \times \boldsymbol{p}$). Since the radial vector $\boldsymbol{r}(x, y, z)$ and the axial vector $\boldsymbol{r} \times \boldsymbol{p}\,(R_x, R_y, R_z)$ transform differently under the symmetry operations of group G, every standard character table normally lists the irreducible representations for the six basis functions for (x, y, z) and (R_x, R_y, R_z) (see Table 6.4).

4. From the characters for the irreducible representations for the molecular vibrations, we find the normal modes. The normal modes for a molecule as defined by Eq. (6.10) are constrained to contain only internal degrees of freedom, and no translations or rotations of the full molecule. Furthermore, the normal modes must be orthogonal to each other.
5. We use the techniques for selection rules (see Section 6.1.8) to find out whether or not each of the normal modes is Raman-active.

It is important to recall that $\Gamma_{\text{vec}}(R)$ is obtained by summing the irreducible representations to which the x, y, and z basis functions belong. If (x, y, z) are the partners of a three-dimensional irreducible representation for T translations, then $\Gamma_{\text{vec}}(R) = \Gamma^T(R)$. If, instead, x, y, and z belong to the same one-dimensional irreducible representation A, then $\Gamma_{\text{vec}}(R) = 3\Gamma^A(R)$. If the x, y, and z basis functions are not given in the character table, $\Gamma_{\text{vec}}(R)$ can be found directly from the trace of the matrix representation for R. All the point group operations are rotations or combination of rotations with inversion. For proper rotations by an angle θ, $\chi_{\text{vec}}(R) = 1 + 2\cos\theta$, so that the trace for the rotation matrix can be always be found directly from the rotation matrix

$$\begin{pmatrix} \cos(\theta) & \sin(\theta) & 0 \\ -\sin(\theta) & \cos(\theta) & 0 \\ 0 & 0 & 1 \end{pmatrix} . \tag{6.11}$$

Improper rotations consist of a rotation followed by a reflection about a horizontal plane resulting in the character $-1 + 2\cos\theta$ where the +1 for a proper rotation goes into −1 for an improper rotation, since z goes into $-z$ upon reflection.

8) The direct product of two IRs means that the characters of the two IRs for each class are multiplied with one another. The representation thus obtained is generally a reducible representation which is then decomposed into IRs.

Considering group D_3, imagine a hypothetical molecule made of three identical atoms at the vertices of the equilateral triangle. We have

	E	$2C_3$	$3\sigma_v$	
$\Gamma^{\text{a.s.}}$	3	0	1	$\Rightarrow A_1 + E$

So that

$$\Gamma_{\text{lat. mode}} = \Gamma^{\text{a.s.}} \otimes \Gamma_{\text{vec}}$$
$$\Gamma_{\text{lat. mode}} = (A_1 + E) \otimes (A_2 + E) = A_1 + 2A_2 + 3E\ . \tag{6.12}$$

From these modes, three modes ($A_2 + E$) are molecular rotations, three modes ($A_2 + E$) are molecular translations (see respective basis functions in Table 6.4) and the other three ($A_1 + E$) are vibrational modes.

6.1.8
Selection Rules

In considering selection rules we always involve some interaction matrix $\mathcal{H}'$ that couples two states ψ_α and ψ_β. If $\mathcal{H}'\psi_\beta$ is orthogonal to ψ_α, then the matrix element $\langle\psi_\alpha|\mathcal{H}'|\psi_\beta\rangle$ vanishes by symmetry;[9] otherwise, the matrix element need not vanish, and the transition from state α to β may occur via $\mathcal{H}'$. Group theory is often invoked to decide whether or not $\langle\psi_\alpha|\mathcal{H}'|\psi_\beta\rangle$ vanishes by symmetry, and this information can be extracted from the character tables. First, we identify the IRs for $\psi_\alpha, \mathcal{H}'$ and ψ_β. Then we multiply their respective characters $\chi_{\mathcal{H}'}(R) \otimes \chi_{\psi_\beta}(R)$. Such a multiplication process can be described by a linear combination of characters coming from different IRs of the group. If this linear combination contains the IR for the ψ_α state,[10] the matrix is nonvanishing by symmetry. Otherwise, $\mathcal{H}'\psi_\beta$ is orthogonal to ψ_α. This rule is applied to obtain the selection rules for the matrix elements occurring in Raman scattering, as discussed in this chapter.

6.2
First-Order Raman Scattering Selection Rules

In Section 4.3.2.7 we described the momentum conservation requirement ($q \sim 0$) for first-order Raman scattering, which goes hand in hand with the translational symmetry in the periodic lattice. Here we derive other symmetry requirements for first-order symmetry-allowed Raman scattering processes for phonons related to the other symmetry elements (rotations, reflections, etc.) of the crystal lattice. Suppose that we have a group G with symmetry elements R and symmetry opera-

9) This means that the integrated function is an odd function of the variables so the implied integration gives a zero value.

10) Or alternatively the representation whose character is the direct product $\psi_\alpha(R) \otimes \chi_{\mathcal{H}'}(R) \otimes \chi_{\psi_\beta}(R)$ contains the totally symmetric IR Γ_1.

tors $\hat{P}_R$. We denote the IRs by Γ_n, where n labels the IR. We can then define a set of basis functions denoted by $|\Gamma_n j\rangle$, with $j = 1, 2, \ldots \ell_j$, where ℓ_j is the dimension of the IR.

As shown in Section 5.4.1, the electromagnetic interaction for electric dipole transitions is given by:

$$\mathcal{H}_{eR} = -\frac{e}{m}\boldsymbol{p}\cdot\boldsymbol{A}\,, \tag{6.13}$$

in which $\boldsymbol{p}$ is the momentum operator of the electron and $\boldsymbol{A}$ is the vector potential of an external electromagnetic field.[11] In the dipole approximation, $\boldsymbol{A}$ (or $\boldsymbol{E}$) which have a much longer wavelength than the unit cell size is considered to be a constant vector within the unit cell, which means that $\boldsymbol{A}$ can be taken out of the matrix element $\langle a|\boldsymbol{p}\cdot\boldsymbol{A}|i\rangle = \langle a|\boldsymbol{p}|i\rangle\cdot\boldsymbol{A}$.

As discussed in the previous section (Section 6.1.8), to have a nonvanishing matrix element $\langle a|\boldsymbol{p}|i\rangle$, we need

$$\Gamma_a \subset \Gamma_{\boldsymbol{p}} \otimes \Gamma_i\,, \tag{6.14}$$

where Γ_i, Γ_a and $\Gamma_{\boldsymbol{p}}$ are the IRs for the initial and intermediate electronic states and for the electron radiation Hamiltonian interaction, respectively. The symbol $A \subset B$ is defined so that A is a subset of B. That is, in the reducible representation of B, we can find the IR for A.

Similarly, the electron–phonon matrix element $\langle b|H_{e\text{-ion}}|a\rangle$ is nonvanishing if

$$\Gamma_b \subset \Gamma_{H_{e\text{-ion}}} \otimes \Gamma_a \subset \Gamma_{H_{e\text{-ion}}} \otimes \Gamma_{\boldsymbol{p}} \otimes \Gamma_i\,, \tag{6.15}$$

if we consider that state $|a\rangle$ here was generated from $|i\rangle$ by $\mathcal{H}_{eR}$. In sequence, the symmetry for the final state in $\langle f|\boldsymbol{p}|b\rangle\langle b|H_{e\text{-ion}}|a\rangle\langle a|\boldsymbol{p}|i\rangle$ has to obey

$$\Gamma_f \subset \Gamma_{\boldsymbol{p}} \otimes \Gamma_b \subset \Gamma_{\boldsymbol{p}} \otimes \Gamma_{H_{e\text{-ion}}} \otimes \Gamma_{\boldsymbol{p}} \otimes \Gamma_i\,, \tag{6.16}$$

which gives the selection rules for state $|f\rangle$being generated from state $|i\rangle$ by the third-order Raman scattering process. The Raman process ends with the electron decaying back to its original state, which means the initial and final electronic states are the same ($|f\rangle \equiv |i\rangle$). Therefore,

$$\Gamma_{\Psi_i} \subset \Gamma_{\boldsymbol{p}} \otimes \Gamma_{H_{e\text{-ion}}} \otimes \Gamma_{\boldsymbol{p}} \otimes \Gamma_{\Psi_i}\,, \tag{6.17}$$

with Γ_{Ψ_i} being the IR for the initial electronic state. This condition is the same as saying that a Raman-active mode has to obey

$$\Gamma_{\boldsymbol{p}} \otimes \Gamma_{H_{e\text{-ion}}} \otimes \Gamma_{\boldsymbol{p}} \supset \Gamma_1\,, \tag{6.18}$$

11) Alternatively, $\mathcal{H}_{eR}$ can also be given by $-e\boldsymbol{r}\cdot\boldsymbol{E}$ (see Section 5.4.1), and then $\boldsymbol{r}$ transforms as a vector.

where Γ_1 is the totally symmetric IR. Since Γ_p pertains to the same IR as the basis functions x, y and z, the condition above is valid if $\Gamma_{H_e\text{-ion}}$ belongs to the same IR as the symmetric combinations of the biquadratic basis functions xx, yy, zz, xy, xz and yz.[12] Therefore, one can identify the Raman-active modes as those pertaining to the same IRs as the biquadratic functions, which are often listed in character tables. Furthermore, the first and second letters in the biquadratic functions denote the polarization directions that the incident and scattered light must have, respectively, in order to observe the phonon pertaining to that IR. For the hypothetical triangular molecule discussed in Section 6.1.7, both the A_1 and E symmetry vibrational modes are Raman-active (see Table 6.4). For this molecule, only the A_1 mode can be seen for incident and scattered light polarized parallel to each other (basis functions $x^2 + y^2$ or z^2). Only the E modes can be seen when the incident and scattered light are cross polarized (basis functions $(x^2 - y^2, xy)$ or (xz, yz)).

6.3 Symmetry Aspects of Graphene Systems

In this section the group theory of graphene systems is summarized to provide a fundamental basis for using group theory to describe the electronic and vibrational properties of sp^2 carbons, previously discussed in Chapters 2 and 3, respectively.

6.3.1 Group of the Wave Vector

Figure 6.2a shows the hexagonal real space structure for monolayer graphene (1-LG) with two nonequivalent atoms per unit cell. The origin in real space is set at the highest symmetry point, that is, at the center of a hexagon, and Figure 6.2a shows the unit vectors defining the rhombic in-plane unit cell, containing the two inequivalent carbon atom sites A and B. Monolayer graphene is an isotropic planar medium described by the 2D space group P6/mm[13] in the Hermann–Mauguin notation.[14] Electrons and phonons at the Γ point both exhibit the symmetries of the point group D_{6h}. The character table for group D_6 is given in Table 6.5 and $D_{6h} = D_6 \otimes C_i$. Here the symbol $\otimes$ represents the so-called direct product,[15]

12) The Raman tensor needs to be a symmetric second rank tensor, and the symmetrized forms of xy, xz and yz are here needed, such as $(xy + yx)/2$, etc.

13) P6/mm denotes a primitive (or simple) lattice, with a six-fold rotational axis, and two mirror planes.

14) Both Hermann–Mauguin and Schoenflies notations are used to describe point group and space group symmetry operations [94].

15) Let $G_A = E, A_2, \ldots, A_{h_a}$ and $G_B = E, B_2, \ldots, B_{h_b}$ be two groups such that all operators A_R commute with all operators B_S. Then the direct product group is written as $G_A \otimes G_B = E, A_2, \ldots, A_{h_a}, B_2, A_2B_2, \ldots, A_{h_a}B_2, \ldots, A_{h_a}B_{h_b}$, where the elements of the direct product group are also indicated.

Table 6.5 Character table for group D_6 (hexagonal)[a] [94].

D_6 (622)			E	C_2	$2C_3$	$2C_6$	$3C_2'$	$3C_2''$
x^2+y^2, z^2		A_1	1	1	1	1	1	1
	R_z, z	A_2	1	1	1	1	−1	−1
		B_1	1	−1	1	−1	1	−1
		B_2	1	−1	1	−1	−1	1
(xz, yz)	(x, y) (R_x, R_y)	E_1	2	−2	−1	1	0	0
(x^2-y^2, xy)		E_2	2	2	−1	−1	0	0

a $D_{6h} = D_6 \otimes i$; $(6/mmm)$ (hexagonal).

which here indicates the direct product of the group D_6 and the group C_i.[16] This is equivalent to adding a horizontal plane of symmetry.[17]

Wave functions away from the Γ point exhibit symmetries lower than D_{6h}, and these lower symmetries are listed in Table 6.6. Character tables for the point groups for all the high symmetry points for monolayer graphene can be found in [94]. This reference also contains extensive information relevant to all types of graphene and sp^2 carbons. More explicitly, the point groups for electron and phonon wavefunctions at other high symmetry points for monolayer graphene are: $3m$[18] for K (K') points, mm for M points, m for T (T') and Σ points, where T (T') and Σ points lie on the line of ΓK (KM) and ΓM, respectively (see Figure 6.2c), and C_1 simply denotes the point group for the general points u in the Brillouin zone that have no special symmetry operations. The groups for wavefunctions at the k point in the Brillouin zone are usually named the *group of the wave vector* (GWV).

When graphene layers are stacked in the AB Bernal structure in real space, carbon atoms A_1 and A_2 on A sites are found one above the other on adjacent layers,

Table 6.6 The space groups and the group of the wave vector point groups for monolayer, N-layer graphene and graphite at all high symmetry points in the Brillouin zone [98].

	Space group	Γ	K (K')	M	T (T')	Σ	u
Monolayer	$P6/mm$	D_{6h}	D_{3h}	D_{2h}	C_{2v}	C_{2v}	C_{1h}
N even	$P\bar{3}m1$	D_{3d}	D_3	C_{2h}	C_2	C_{1v}	C_1
N odd	$P\bar{6}m2$	D_{3h}	C_{3h}	C_{2v}	C_{1h}	C_{2v}	C_{1h}
N infinite	$P6_3/mmc$	D_{6h}	D_{3h}	D_{2h}	C_{2v}	C_{2v}	C_{1h}

16) C_i has two symmetry elements, the identity E and the inversion i.

17) $C_2 i = \sigma_h$, and $C_2' i = \sigma_v$, where σ_h and σ_v are, respectively, horizontal and vertical mirror plane operations when we put the C_6 axis in the vertical direction.

18) $3m$ denotes three-fold rotational and mirror plane symmetry.

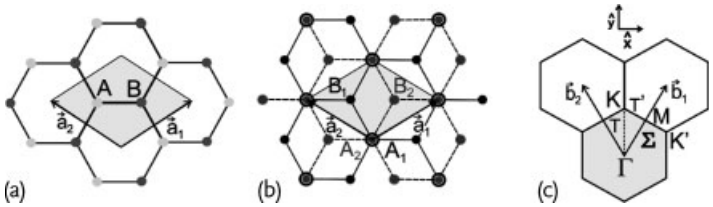

Figure 6.2 (a) The real space top-view of the setting for the unit cell for monolayer graphene, showing the nonequivalent A and B atoms and unit cell vectors $\boldsymbol{a}_1$ and $\boldsymbol{a}_2$. (b) The real space top-view of the setting for the unit cell for bilayer graphene. Light and dark gray dots in (a) denote A and B atoms in 1-LG. Large gray circles represent A atoms which are above one another in bilayer graphene. Small black and gray dots represent B atoms on the lower and upper layers, respectively. Thus the A atoms are above one another on adjacent layers, but the B atoms are instead staggered on adjacent layers for Bernal stacking. (c) The hexagonal reciprocal space showing high symmetry points and lines [98].

while the B atoms alternate between the B_1 and B_2 sites on adjacent layers, as seen in Figure 6.2b.[19)]

The real space unit cell for bilayer graphene with AB Bernal stacking is shown in Figure 6.2b, and this is the fundamental unit cell for all N even-layer graphenes, including graphite in the large N limit. All N odd-layer graphenes can be considered as having a single graphene layer, flanked by bilayer unit cells on either side. The main symmetry operation distinguishing the point groups between even and odd layers is the horizontal mirror plane symmetry, which is absent for N even, and the inversion operation, which is absent for N odd. The space groups, and the group of the wave vector for all the high symmetry points in monolayer graphene, even and odd layer graphenes ($N > 1$), and for graphite in the large N limit are listed in Table 6.6. The GWV for N-layer graphenes are subgroups of the GWV for single-layer graphene. The direct product between the space group for N even with no translations and the space group for N odd with no translations gives the space group for the monolayer graphene GWV with no translations, that is,

$$\{G_{\text{even}}|0\} \otimes \{G_{\text{odd}}|0\} = \{G_{1-LG}|0\}, \tag{6.19}$$

which can be seen when carrying out the direct product operations between these groups. Graphite belongs to the $P6_3/mmc$ ($D_{6h}{}^4$) nonsymmorphic space group[20)] while the space group for monolayer graphene is $P6/mm$ and is symmorphic. For graphite, the GWV is $P6_3/mmc$ at the Γ point. However, the group of the wave vector for graphite at high symmetry points in the BZ is isomorphic to the GWV of monolayer graphene, but they differ fundamentally for some classes where a

19) For three layers, the B_1 and B_3 appear at the same in-plane positions, while the B_2 atom is in a staggered location as shown in Figure 6.2b. Such stacking of adjacent planes is called ABAB stacking.

20) Depending on the existence or not of a spiral (or chiral) operation in the crystal symmetry, the space group is divided into nonsymmorphic and symmorphic space groups. Most of the space groups that we discuss in solid state textbooks are symmorphic space groups, for which the translation operations and the point group operations commute. For nonsymmorphic groups, translations and point group operations do not commute.

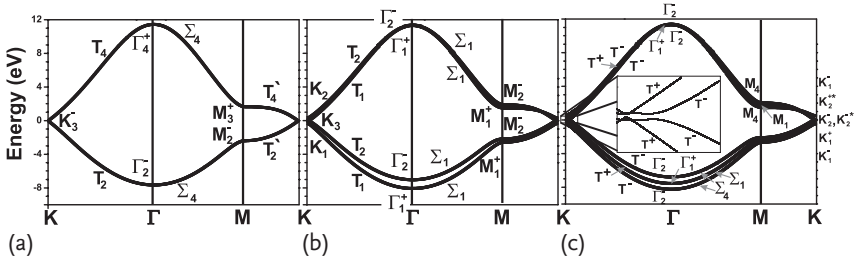

Figure 6.3 The electronic dispersion for the π electrons, calculated by DFT and using the irreducible representations (Γ_π), are shown for (a) monolayer, (b) bilayer and (c) trilayer graphene along the KΓMK directions [98].

translation of $c/2$ is present in the symmetry operations in graphite, and in this way graphite is homomorphic to monolayer graphene.

6.3.2
Lattice Vibrations and π Electrons

The group theoretical representations for lattice vibrations ($\Gamma_{\text{lat. mode}}$) and for π electron states (Γ_π) are given by the direct products as $\Gamma_{\text{lat. mode}} = \Gamma^{\text{a.s.}} \otimes \Gamma^{\text{vec}}$ and $\Gamma_\pi = \Gamma^{\text{a.s.}} \otimes \Gamma^{z}$, respectively, where $\Gamma^{\text{a.s.}}$ is the atom sites equivalence representation,[21] and Γ^{vec} is the representation for the vectors x, y and z [94].[22] For Γ_π we use only Γ^z, which is the irreducible representation for the vector z, since π electrons in graphene are formed by p_z electronic orbitals normal to the layer planes. The irreducible representations for all high symmetry points and lines in the first BZ for $\Gamma_{\text{lat. mode}}$ are found in Table 6.7. The corresponding results for Γ_π are found in Table 6.8 (see Section 6.3.6 for the notation conversion from space group to point group). Furthermore, Table 6.8 shows that the π electrons in monolayer graphene are degenerate at the K (Dirac) point, as obtained by theory [31]. Figure 6.3a, b and c show the electronic structure of monolayer, bilayer and trilayer graphene, respectively, calculated via density functional theory (DFT) [98, 217]. The symmetry assignments of the different electronic branches shown in Figure 6.3 were made according to the symmetries of the DFT projected electronic density of states [98].

21) The atom sites equivalence representation is a reducible representation of the point group of the unit cell, in which each value for $\Gamma^{\text{a.s.}}$ corresponds to the number of atoms that do not change their position by each symmetry operation. For the mirror symmetry operation, the number of atoms on the mirror corresponds to that value. For rotational operations, the number of atoms on the rotational axis corresponds to that value.

22) If you look at the character table, you sometimes see simple functions such as x, y, z or xy, etc., which can correspond to an irreducible representation. If this is not the case, you need to find by yourself which irreducible representation corresponds to x, y and z.

Table 6.7 The $\Gamma_{\text{lat. mode}}$ wave vector point-group irreducible representations for mono- and N-layer graphene at all distinct symmetry points in the BZ [98].

	Monolayer	**N even**	**N odd**
Γ	$\Gamma_2^- + \Gamma_5^- + \Gamma_4^+ + \Gamma_6^+$	$N(\Gamma_1^+ + \Gamma_3^+ + \Gamma_2^- + \Gamma_3^-)$	$(N-1)\Gamma_1^+ + (N+1)\Gamma_2^- + (N+1)\Gamma_3^+ + (N-1)\Gamma_3^-$
K	$K_1^+ + K_2^+ + K_3^+ + K_3^-$	$N(K_1 + K_2 + 2K_3)$	$NK_1^+ + NK_1^- + [f(N)+2]K_2^+ + [f(N-2)]K_2^{+*}$ $+NK_2^- + (N-1)K_2^{-*}$ [a]
M	$M_1^+ + M_2^+ + M_3^+ + M_2^- + M_3^- + M_4^-$	$N(2M_1^+ + M_2^+ + M_1^- + 2M_2^-)$	$2NM_1 + (N-1)M_2 + (N+1)M_3 + 2NM_4$
$T\,(T')$	$2T_1 + T_2 + 2T_3 + T_4$	$3N(T_1 + T_2)$	$(3N+1)10T^+ + (3N-1)T^-$
Σ	$2\Sigma_1 + 2\Sigma_3 + 2\Sigma_4$	$N(4\Sigma_1 + 2\Sigma_2)$	$2N\Sigma_1 + (N-1)\Sigma_2 + (N+1)\Sigma_3 + 2N\Sigma_4$
u	$4u^+ + 2u^-$	$6Nu$	$(3N+1)u^+ + (3N-1)u^-$

a Where $f(N) = \sum_{m=0}^{\infty}[\Theta(N-4m-2) + 3\Theta(N-4m-4)]$, in which $\Theta(x)$ is equal to 0 if $x < 0$, and equal to 1 otherwise.

Table 6.8 The Γ_π wave vector point-group irreducible representations for mono- and N-layer graphene at all high symmetry points in the BZ [98].

	Monolayer	**N even**	**N odd**
Γ	$\Gamma_2^- + \Gamma_4^+$	$N(\Gamma_1^+ + \Gamma_2^-)$	$(N-1)\Gamma_1^+ + (N+1)\Gamma_2^-$
$K\,(K')$	K_3^-	$\frac{N}{2}(K_1 + K_2 + K_3)$	$(\frac{N-1}{2})K_1^+ + (\frac{N+1}{2})K_1^- + g(N)K_2^{+*}(K_2^+) + g(N-2)(K_2^+)(K_2^{+*}) + g(N)K_2^- + g(N+2)K_2^{-*}$ [a]
M	$M_3^+ + M_2^-$	$N(M_1^+ + M_2^-)$	$(N-1)M_1 + (N+1)M_4$
$T\,(T')$	$T_2 + T_4$	$N(T_1 + T_2)$	$(N-1)T^+ + (N+1)T^-$
Σ	$2\Sigma_4$	$2N\Sigma_1$	$(N-1)\Sigma_1 + (N+1)\Sigma_4$
u	$2u^-$	$2Nu$	$(N-1)u^+ + (N+1)u^-$

a Where $g(N) = \sum_{m=0}^{\infty} \Theta\,(N-4m-2)$, in which $\Theta\,(x)$ is equal to 0 if $x < 0$ and equal 1 otherwise.

Trilayer graphene with ABA Bernal stacking belongs to the D_{3h} point group, and Figure 6.3c shows its electronic dispersion. The group of the wave vector for the K point of trilayer graphene is isomorphic to the point group C_{3h}. In Tables 6.7 and 6.8, K_2^+ and K_2^{+*} are the two one-dimensional representations comprising the K_2^+ representation, and $*$ denotes the complex conjugate. The same applies to the K_2^- representation. The irreducible representations for the electronic bands are given by $\Gamma_\pi^K = K_1^+ + 2K_1^- + K_2^{+*} + K_2^- + K_2^{-*}$ for the K point and $\Gamma_\pi^{K'} = K_1^+ + 2K_1^- + K_2^+ + K_2^{-*} + K_2^-$ for the K′ point. Although time reversal symmetry can imply degeneracy between the complex conjugate representations for cyclic groups, in graphene the complex conjugation operation also takes K into the K' point and vice versa. Consequently, there are no degenerate bands at the K (K') point, in agreement with *tight-binding* calculations. These calculations include the γ_2 and γ_5 next-nearest layer coupling parameters in describing $E(k)$ for graphite [97, 221], which are necessary to describe the Fermi surface for graphite. An energy gap at the K point is obtained for both DFT calculations and *ab initio* calculations (see the inset of Figure 6.3c and more details in [98]).

6.3.3
Selection Rules for the Electron–Photon Interaction

In this section we discuss the selection rules for the electron–photon interaction in the dipole approximation, with emphasis given to the high symmetry lines T and T' in the electronic dispersion (see Figure 6.2c). These high symmetry T and T' lines along the ΓK and KM directions in reciprocal space, respectively, are important for Raman spectroscopy.[23] In fact, the light absorption up to 3 eV occurs mostly along the T, T' lines but there is also some absorption at general u points near the K (K') point in the case of graphene.

In Table 6.9, we show the direct products for three irreducible representations for the final state, the electron–photon perturbation, and the initial state $\Gamma_f \otimes \Gamma_{\boldsymbol{p}} \otimes \Gamma_i$ in the column of the absorption matrix element $W(k)$. Knowing the symmetry of the initial and final states, and the irreducible representation that generates the basis function of the light polarization vector (x, y or z), group theory can be used to calculate whether $W(k)$ is zero or not by only using the character table. The results are summarized in Table 6.9 considering the graphene layers to be in the (x, y) plane and the light propagating along the z direction.

It is important to highlight some results given in Table 6.9 where the symbol $x \in T_3$ tells us that x belongs to the IR for T_3. The column for $W(k)$ gives the selection rules for the electron–photon interaction in terms of the direct products of the relevant irreducible representations. Along the T line, absorption by visible light has to couple T_2 and T_4 π electron symmetries which have the same basis functions of x and y as for monolayer graphene (see Figure 6.3a). For the T line

23) In the Raman spectroscopy of carbon nanotubes, the Raman signal or intensity depends on the corresponding one-dimensional Brillouin zone lying along the ΓK or KM directions. This gives a so-called type I and II dependence for semiconducting SWNTs, respectively, for Raman spectroscopy [222].

Table 6.9 Selection rules for the electron–photon interaction $W(k)$ with $\hat{x}$ and $\hat{y}$ light polarization in monolayer, bilayer and trilayer graphene (see Figure 6.2c for definitions of $\hat{x}$ and $\hat{y}$). For N even and N odd, the selection rules are the same as for bilayer and trilayer graphene, respectively. T_1 to T_4 are IRs for the GWV for the T point [98]. Here $x \in T_3$ means x transforms according to the IR T_3. For notation see Section 6.3.6.

	BZ point	Polarization	$W(k)$
Monolayer	T	$x \in T_3$	$T_2 \otimes T_3 \otimes T_4$ nonzero
		$y \in T_1$	$T_2 \otimes T_1 \otimes T_4$ zero
	u	$x, y \in u^+$	$u^- \otimes u^+ \otimes u^-$ nonzero
Gated monolayer	T	$x \in T_2$	$T_1 \otimes T_2 \otimes T_2$ nonzero
		$y \in T_1$	$T_1 \otimes T_1 \otimes T_2$ zero
	u	$x, y \in u$	$u \otimes u \otimes u$ nonzero
Bilayer (N-even)	T	$x \in T_2$	$T_1 \otimes T_2 \otimes T_1$ zero
			$T_1 \otimes T_2 \otimes T_2$ nonzero
			$T_2 \otimes T_2 \otimes T_2$ zero
		$y \in T_1$	$T_1 \otimes T_1 \otimes T_1$ nonzero
			$T_1 \otimes T_1 \otimes T_2$ zero
			$T_2 \otimes T_1 \otimes T_2$ nonzero
	u	$x, y \in u$	$u \otimes u \otimes u$ nonzero
Biased bilayer	T	$x, y \in T$	$T \otimes T \otimes T$ nonzero
	u	$x, y \in u$	$u \otimes u \otimes u$ nonzero
Trilayer (N-odd)	T	$x, y \in T^+$	$T^+ \otimes T^+ \otimes T^+$ nonzero
			$T^+ \otimes T^+ \otimes T^-$ zero
			$T^- \otimes T^+ \otimes T^-$ nonzero
	u	$x, y \in u^+$	$u^+ \otimes u^+ \otimes u^+$ nonzero
			$u^+ \otimes u^+ \otimes u^-$ zero
			$u^- \otimes u^+ \otimes u^-$ nonzero

direction along $\hat{y}$, the only allowed absorption is for light polarized along the $\hat{x}$ direction (T_3). For incident light polarization along the $\hat{y}$ direction (T_1), no absorption will occur along the KΓ direction along the k_y axis, giving rise to an optical absorption anisotropy for monolayer graphene [83, 220].

Bilayer graphene contains four electronic bands along the T line, belonging to two T_1 and two T_2 irreducible representations. The four possible transitions are illustrated in Figure 6.4 (a,b). In this case, both x and y polarized light can be absorbed. Trilayer graphene will have more possibilities for light-induced transitions, since there are more possibilities between the three π and three π^*-bands. Along the T (T') direction, there are two T^+ and four T^--bands for trilayer graphene, giving rise to five possible transitions (see Table 6.9), as shown in Figure 6.4c.

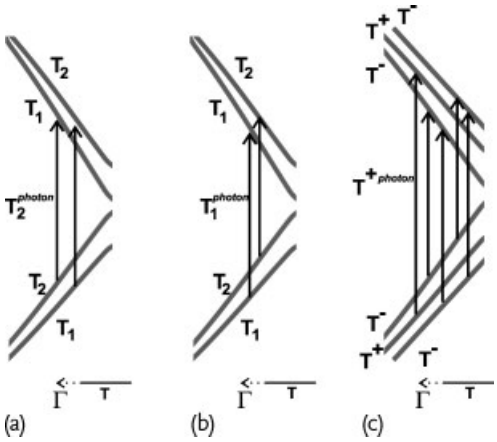

Figure 6.4 (a,b) Schematic electron dispersion of bilayer graphene along the KΓ direction showing the possible transition induced by (a) a photon with T_2 symmetry (x polarization) and (b) a T_1 photon (y polarization). (c) The electronic dispersion of trilayer graphene showing the five possible transitions by light absorption [98].

6.3.4
Selection Rules for First-Order Raman Scattering

The first-order Raman scattering process is limited to phonons at the center of the BZ (Γ point) due to the momentum conservation requirement (phonon wave vector $q = 0$). In monolayer graphene, although there are three optical modes at the Γ point, two (the LO and iTO) are degenerate and one (the oTO) is not Raman-active. The first-order Raman spectra is therefore composed of the G-band vibrational mode, which is doubly degenerate at the Γ point with Γ_6^+ (or E_{2g}) symmetry.[24] The Raman-active modes of N graphene layers which depend on N ($N > 1$) (without the acoustic modes) are:

$$\begin{aligned} \Gamma^{\text{Raman}} &= N(\Gamma_3^+ + \Gamma_1^+), \text{ for } N \text{ even} \\ \Gamma^{\text{Raman}} &= N\Gamma_3^+ + (N-1)(\Gamma_3^- + \Gamma_1^+), \text{ for } N \text{ odd.} \end{aligned} \tag{6.20}$$

For an even number of graphene layers, the G-band belongs to the Γ_3^+ irreducible representation. There is a low frequency Γ_3^+ mode with a frequency depending on the number of layers (35–53 cm^{-1}) [223]. Two new Raman-active modes near $\sim 80\,\text{cm}^{-1}$ and $\sim 900\,\text{cm}^{-1}$ appear belonging to the Γ_1^+ irreducible representations [223, 224]. For an odd number of graphene layers, the G-band is assigned to a combination of Γ_3^+ and Γ_3^- representations, and also the lower wavenumber component is Raman-active by a Γ_1^+ representation.

24) Although the space group notation, where the IRs are labeled by the BZ point label, is more complete, it is common in the Raman spectroscopy literature to use the notation from the isomorphic point groups, since only the Γ point ($q \sim 0$) is usually relevant. For the D_{6h} point group notation, Γ_6^+ corresponds to the E_{2g} IR. Information about the space group to point group notation conversion is found in Section 6.3.6.

6.3.5
Electron Scattering by $q \neq 0$ Phonons

The electron–phonon (el–ph) interaction is calculated from the coupling of the initial and final electron wave functions to the phonon eigenvector [8, 203] using a phonon-induced deformation potential. Therefore, the selection rules for the el–ph processes are obtained by taking the direct product of the symmetries of the initial and final electronic states and the symmetry of the phonon involved in the el–ph process. The allowed el–ph scattering processes for monolayer, gated monolayer, bilayer, biased bilayer and trilayer graphene along the $K\Gamma$ and KM directions (T and T' lines, respectively) and at a generic u point are summarized in Table 6.10.

6.3.6
Notation Conversion from Space Group to Point Group Irreducible Representations

Here we derive the Γ_π and $\Gamma_{\text{lat. mode}}$ representations for the electrons and phonons for all points in the first BZ of multi-layer graphene maintaining the notation of the space group (SG) for the irreducible representations. The conversion to point group (PG) representations is obtained by considering that (a) the superscript sign

Table 6.10 Allowed processes for electron–phonon scattering for monolayer, bilayer and trilayer graphene along the T and T' lines and at a generic u point for each phonon symmetry. For N even and N odd graphenes, the selection rules are the same as for bilayer and trilayer graphene, respectively. The table also includes entries for a gated monolayer and a biased bilayer [98].

	BZ point	Phonon	Allowed scattering
Monolayer	$T\,(T')$	T_1	$T_2 \to T_2, T_4 \to T_4$
		T_3	$T_2 \to T_4$
	u	u^+	$u^- \to u^-$
Gated monolayer	$T\,(T')$	T_1	$T_1 \to T_1, T_2 \to T_2$
		T_2	$T_1 \to T_2$
	u	u	$u \to u$
Bilayer (N-even)	$T\,(T')$	T_1	$T_1 \to T_1, T_2 \to T_2$
		T_2	$T_1 \to T_2$
	u	u	$u \to u$
Biased bilayer	$T\,(T')$	T	$T \to T$
	u	u	$u \to u$
Trilayer (N-odd)	$T\,(T')$	T^+	$T^+ \to T^+, T^- \to T^-$
		T^-	$T^+ \to T^-$
	u	u^+	$u^+ \to u^+, u^- \to u^-$
		u^-	$u^+ \to u^-$

Table 6.11 Example of the irreducible representation notation conversion from the Γ point space group (SG) to the D_{3h} and D_{3d} point groups (PG), and from the K point space group (SG) to the C_{3h} and D_3 point groups (PG) [98].

Γ point				K point			
D_{3h}		D_{3d}		C_{3h}		D_3	
SG	PG	SG	PG	SG	PG	SG	PG
Γ_1^+	A'_1	Γ_1^+	A_{1g}	$K_1{}^+$	A'	K_1	A_1
Γ_1^-	A''_1	Γ_1^-	A_{1u}	$K_1{}^-$	A''	K_2	A_2
Γ_2^+	A'_2	Γ_2^+	A_{2g}	$K_2{}^+$	E'	K_3	E
Γ_2^-	A''_2	Γ_2^-	A_{2u}	$K_2{}^{+*}$	E'^*		
Γ_3^+	E'	Γ_3^+	E_g	$K_2{}^-$	E''		
Γ_3^-	E''	Γ_3^-	E_u	$K_2{}^{-*}$	E''^*		

"+" or "−" applies if the character of the horizontal mirror plane (σ_h) or the inversion operation (i) is positive or negative, respectively; (b) the subscript number is given following the order of the point group irreducible representations; (c) two representations can only have the same subscript number if they both have superscripts with positive or negative signs. As an example, we give in Table 6.11 the Γ point space group notation conversion to the D_{3h} (N-odd) and D_{3d} (N-even) point groups and for the K point space group to the C_{3h} (N-odd) and D_3 (N-even) point groups.

6.4 Symmetry Aspects of Carbon Nanotubes

The nanotube physical properties depend on how the graphene sheet is rolled up, and from a symmetry point of view, two types of nanotubes can be formed, namely the symmorphic achiral armchair or zigzag tubes, as shown in Figure 6.5a,b, respectively, and the nonsymmorphic chiral tubes, shown in Figure 6.5c.[25] Simply put, for the symmorphic groups, the translations and rotations can be decoupled, while for nonsymmorphic the rotations also contain translations, such as screw rotations along the tube axis [94]. We note in Figure 6.5 that each nanotube has a cap at either end of the nanotube. Because of the small diameter of a carbon nanotube ($\sim$1 nm) and the large length-to-diameter ratio ($> 10^4$), it is assumed that the nanotube length is much larger than its diameter, so that the nanotube ends (see Figure 6.5) can be neglected when discussing the electronic and lattice properties of the nanotubes. Thus from a symmetry standpoint, a carbon nanotube is a one-dimensional crystal with a translation vector $\boldsymbol{T}$ along the cylinder axis and

25) If we take the smallest unit cell consisting of two carbon atoms for achiral nanotubes, we should consider the screw rotation. In general, the symmetry selection rule depends on the shape of the unit cell. The smallest unit cell is not always the best for understanding the relevant physics.

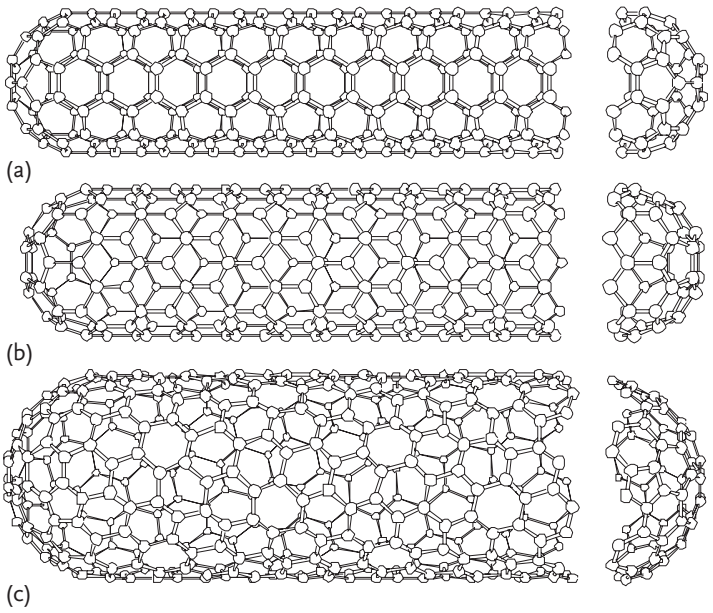

Figure 6.5 Schematic theoretical model for the three different types of single-wall carbon nanotubes: (a) the "armchair" nanotube, (b) the "zigzag" nanotube, and (c) the "chiral" nanotube. The actual nanotubes shown in the figure correspond to (n, m) values of (a) (5, 5), (b) (9, 0), and (c) (10, 5). See text for more information [31].

a small number of carbon hexagons associated with the circumferential direction. The nanotube structure can be considered as a folded graphene defined by the (n, m) indices, as discussed in Section 2.3.1. In this section we give more details that are important for the description of the eigenvectors and selection rules for nanotubes.

6.4.1 Compound Operations and Tube Chirality

All multiples of the translation vector $\boldsymbol{T}$ will be a translational symmetry operation of the nanotube [225]. However, to be more general, it is necessary to consider that any lattice vector

$$\boldsymbol{t}_{p,q} = p\,\boldsymbol{a}_1 + q\,\boldsymbol{a}_2, \tag{6.21}$$

with p and q integers, of the unfolded graphene layer will also be a symmetry operation of the nanotube. In fact, the symmetry operation that arises from $\boldsymbol{t}_{p,q}$ will appear as a screw translation of the nanotube. Screw translations are combinations of a rotation by an angle ϕ (R_ϕ) and a translation $\boldsymbol{\tau}$ in the axial direction of the nanotube. The screw translation can be written as $\{R_\phi|\tau\}$, using a notation common for space group operations [31, 94].

The translation vector from $\boldsymbol{t}_{p,q}$ can also be written in terms of components of the nanotube lattice vectors, $\boldsymbol{T}$ and $\boldsymbol{C}_h$, as

$$\boldsymbol{t}_{p,q} = \boldsymbol{t}_{u,v} = \frac{1}{N}\left(u\boldsymbol{C}_h + v\boldsymbol{T}\right), \tag{6.22}$$

where u and v are given by:

$$u = \frac{(2n+m)p + (2m+n)q}{d_R} \tag{6.23}$$

and

$$v = mp - nq\,. \tag{6.24}$$

N and d_R have been defined in Section 2.3.1 (see Table 2.1). Both u and v in Eqs. (6.23) and (6.24), respectively, are integer numbers which can assume either negative or positive values.

The screw translation of the nanotube $\boldsymbol{t}_{u,v}$ which is associated with the graphene lattice vectors can then be written using the space group notation as:

$$\boldsymbol{t}_{u,v} = \{C_N^u|v\,T/N\}\,, \tag{6.25}$$

where C_N^u is a rotation of u by $(2\pi/N)$ around the nanotube axis, and $\{E|v\,T/N\}$ is a translation of $v\,T/N$ along the nanotube axis, with T being the magnitude of the primitive translation vector $\boldsymbol{T}$ along the tube axis. It is clear that if a screw vector $\{C_N^u|v\,T/N\}$ is a symmetry operation of the nanotube, then the vectors $\{C_N^u|v\,T/N\}^s$, for any integer value of s, are also symmetry operations of the nanotube. The number of hexagons in the unit cell N assumes the role of the "order" of the screw axis, since the symmetry operation $\{C_N^u|v\,T/N\}^N = \{E|v\,T\}$, where E is the identity operator, and $v\boldsymbol{T}$ is a pure translation of the nanotube.

The nanotube structure can be obtained from a small number of atoms (between 2 and $2N$) by using any choice of two independent noncolinear screw vectors, such as $\{C_N^{u_1}|v_1\,T/N\}$ and $\{C_N^{u_2}|v_2\,T/N\}$. Here noncolinear vectors are defined such that there does not exists a pair of integers s and l except for 1, which satisfy $lu_1 = su_2 + \lambda N$, and $lv_1 = sv_2 + \gamma\,T$, where λ and γ are two arbitrary integers [135].

When $\boldsymbol{T}$ is specified, a screw vector $C_N^u|0$ for p and q which satisfies $v = mp - nq = 1$ for an (n, m) nanotube, generates N carbon atoms in the 1D unit cell. This screw vector is called a *symmetry vector* R [31]. To better illustrate the action of the symmetry vector $\boldsymbol{R}$, we show in Figure 6.6 a diagram of the screw vector applied to the (4, 2) nanotube. The dark atoms in the bottom represent a two-atom motif. We also show in Figure 6.6 another set of dark atoms which is equivalent to this motif due to a rotation of $2\pi/d$, with $d = 2$, around the nanotube axis. The dark gray helix of atoms is composed of the atoms in the nanotube unit cell which can be obtained by consecutive applications of the screw vector $\boldsymbol{R}$ to the atoms in the motif, while the other atoms are obtained by successive operations of the screw vector $\boldsymbol{R}$ followed by a pure translation which brings the motif back to the original unit cell [135].

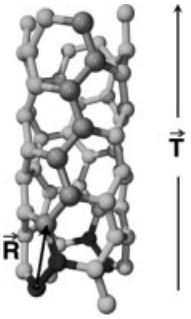

Figure 6.6 Unit cell of the (4,2) nanotube, with its 28 atoms. The dark gray atoms can be directly obtained by the application of the $\boldsymbol{R}$ vector, while the other atoms can be obtained from the latter by applying other symmetry operations, such as the translation vector $\boldsymbol{T}$ [135].

6.4.2
Symmetries for Carbon Nanotubes

The chiral nanotube symmetry operations can be separated into two sets [135]. The first set, which we shall call the symmorphic set, is formed by the translation operations of the nanotube and the point group operations. This symmorphic set forms a sub-group of the total space-group of the nanotube, and thus it can be used to obtain some of the symmetry-related properties. To obtain the point group of the nanotube, the nanotube can be rotated by an angle $2\pi/d$ (called the C_d operation) without changing its structure where $d = \mathrm{gcm}(n, m)$ and gcm denotes the greatest common multiplier. Therefore, the C_d operation is a point group operation of the nanotube. Also, by choosing an axis perpendicular to the nanotube axis, the rotation by π around this axis (C_2' or C_2'') will also be a symmetry operation of the nanotube, as shown in Figure 6.7a. There are two different classes of rotations perpendicular to the nanotube axis (C_2' and C_2''). For one of the classes (C_2'), the axis goes through the center of bonds between two equivalent atoms (shown in Figure 6.7a). For the other class (C_2''), the axis goes through the centers of the hexagons.[26] The point group of the nanotube is thus obtained as the axial point group D_d.[27] The second set of symmetry operations, which we shall refer to as the nonsymmorphic set, is formed by the compound operations of the space group of the nanotube, which cannot be decomposed into pure translations of multiples of $\boldsymbol{T}$ and point group operations. All the screw vectors $\boldsymbol{t}_{u,v}$, with the exception of multiples of $\boldsymbol{T}$ and $\boldsymbol{C}_h/d$, are part of this set of operations [135].

Both armchair (n, n) and zigzag $(n, 0)$ carbon nanotubes exhibit all the symmetry operations that were observed for chiral nanotubes, namely the screw axes $\{C_N^u|v\,T/N\}^s$, where $N = 2n$, the rotation around the nanotube axis C_d, where $d = n$, and the rotations perpendicular to the nanotube axis C_2' and C_2''. However, achiral nanotubes also exhibit other symmetry operations, such as inversion centers as well as mirror planes and glide planes. The horizontal mirror plane σ_h and one of the vertical mirror planes σ_v are shown in Figure 6.7b,c, respectively. There

26) The C_2'' axis of the nanotube corresponds to the C_6 axis in the case of flat graphene.
27) The label D_d means that the group has one C_d rotational operation about the z axis and $2d$ C_2 rotational operations in the xy plane.

is also an inversion center at the intersection of the σ_h plane and the nanotube axis. The glide planes are represented by $\{\sigma_v|T/2\}$.

For chiral tubes, at the Γ point the GWV exhibits the symmetries of the D_N point group [135], for which the character table is shown in Table 6.12. The symmetry properties of general nanotube wave vectors $0 < k < \pi/T$ can be fully described by using the C_N group. In Table 6.13, we show the character table for the irreducible representations of the C_N point group. There are $[(N/2)-1]$ representations which are doubly degenerate due to time reversal symmetry. For $k = \pi/T$ and $k = -\pi/T$, which can be translated into each other by a reciprocal lattice vector $\kappa_2 = 2\pi/T$, the group of the wave vector is also isomorphic to D_N.

For achiral tubes, at the Γ point the GWV is isomorphic to D_{2nh}. The character table for group D_{2nh} is shown in Table 6.14, where the C_{2n} classes correspond to the screw vectors of the nanotube, while the σ'_v and σ''_v classes correspond, respectively, to mirror and glide planes containing the nanotube axis [135]. For $0 < k < \pi/T$ the only symmetry operations which maintain k invariant are the screw vectors and the mirror and glide planes which contain the nanotube axis (σ'_v and σ''_v). The GWV will then be isomorphic to the C_{2nv} point group, for which the character table is shown in Table 6.15. In the case of the (3,3) nanotube (see Figure 6.7b,c), the group of the wave vector at a general point $0 < k < \pi/T$ is isomorphic to the C_{6v} point group, while at $k = 0$ and $k = \pi/T$ the group of the wave vector is isomorphic to the D_{6h} point group [94, 135].

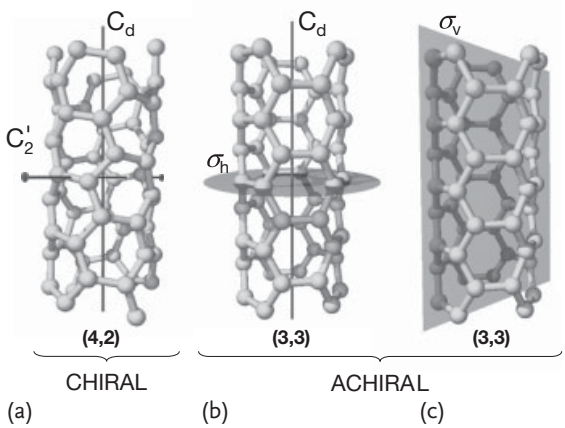

Figure 6.7 (a) Unit cell of the chiral (4,2) nanotube, showing the C_d rotation around the nanotube axis with $d = 2$, and one of the C'_2 rotations perpendicular to the tube axis. A different class of rotations (C''_2), which is also present in chiral and achiral nanotubes, is not shown here. (b) A section of an achiral armchair (3,3) nanotube is shown along with the horizontal mirror plane σ_h and the symmetry operation C_d with $d = 3$. (c) The same (3,3) armchair nanotube is shown along with one of the vertical mirror planes σ_v [135].

Table 6.12 Character table for the group of the wave vectors $k = 0$ and $k = \pi/T$ for chiral tubes. This group is isomorphic to the point group D_N.

D_N	$\{E\|0\}$	$2\{C_N^u\|\nu T/N\}$	$2\{C_N^u\|\nu T/N\}^2$	...	$2\{C_N^u\|\nu T/N\}^{(N/2)-1}$	$\{C_N^u\|\nu T/N\}^{N/2}$	$(N/2)\{C_2'\|0\}$	$(N/2)\{C_2''\|0\}$
A_1	1	1	1	...	1	1	1	1
A_2	1	1	1	...	1	1	-1	-1
B_1	1	-1	1	...	$(-1)^{(N/2-1)}$	$(-1)^{N/2}$	1	-1
B_2	1	-1	1	...	$(-1)^{(N/2-1)}$	$(-1)^{N/2}$	-1	1
E_1	2	$2\cos 2\pi/N$	$2\cos 4\pi/N$	...	$2\cos 2(N/2-1)\pi/N$	-2	0	0
E_2	2	$2\cos 4\pi/N$	$2\cos 8\pi/N$	...	$2\cos 4(N/2-1)\pi/N$	2	0	0
$\vdots$	$\vdots$	$\vdots$	$\vdots$	$\vdots$	$\vdots$	$\vdots$	$\vdots$	$\vdots$
$E_{(N/2-1)}$	2	$2\cos 2(N/2-1)\pi/N$	$2\cos 4(N/2-1)\pi/N$	...	$2\cos 2(N/2-1)^2\pi/N$	$2\cos(N/2-1)\pi$	0	0

Table 6.13 Character table for the group of the general wave vector $0 < k < \pi/T$ for chiral nanotubes. This group is isomorphic to the point group C_N. The $\pm$ signs label the different 1D irreducible representations ($\mathbb{E}$) with characters which are complex conjugates of each other[a]. These representations are degenerate due to time reversal symmetry [135].

C_N	$\{E\|0\}$	$\{C_N^u\|\nu T/N\}^1$	$\{C_N^u\|\nu T/N\}^2$	$\cdots$	$\{C_N^u\|\nu T/N\}^\ell$	$\cdots$	$\{C_N^u\|\nu T/N\}^{N-1}$
A	1	1	1	$\cdots$	1	$\cdots$	1
B	1	-1	1	$\cdots$	$(-1)^\ell$	$\cdots$	-1
$\mathbb{E}_{\pm 1}$	$\left\{\begin{matrix}1\\1\end{matrix}\right.$	$\left.\begin{matrix}\epsilon\\ \epsilon^*\end{matrix}\right\}$	ϵ^2 ϵ^{*2}	$\cdots$	ϵ^ℓ $\epsilon^{*\ell}$	$\cdots$	$\left.\begin{matrix}\epsilon^{N-1}\\ \epsilon^{*(N-1)}\end{matrix}\right\}$
$\mathbb{E}_{\pm 2}$	$\left\{\begin{matrix}1\\1\end{matrix}\right.$	$\left.\begin{matrix}\epsilon^2\\ \epsilon^{*2}\end{matrix}\right\}$	ϵ^4 ϵ^{*4}	$\cdots$	$\epsilon^{2\ell}$ $\epsilon^{*2\ell}$	$\cdots$	$\left.\begin{matrix}\epsilon^{2(N-1)}\\ \epsilon^{*2(N-1)}\end{matrix}\right\}$
$\vdots$	$\vdots$	$\vdots$	$\vdots$	$\vdots$	$\vdots$	$\vdots$	$\vdots$
$\mathbb{E}_{\pm(\frac{N}{2}-1)}$	$\left\{\begin{matrix}1\\1\end{matrix}\right.$	$\left.\begin{matrix}\epsilon^{\frac{N}{2}-1}\\ \epsilon^{*\frac{N}{2}-1}\end{matrix}\right\}$	$\epsilon^{2(\frac{N}{2}-1)}$ $\epsilon^{*2(\frac{N}{2}-1)}$	$\cdots$	$\epsilon^{\ell(\frac{N}{2}-1)}$ $\epsilon^{*\ell(\frac{N}{2}-1)}$	$\cdots$	$\left.\begin{matrix}\epsilon^{(N-1)(\frac{N}{2}-1)}\\ \epsilon^{*(N-1)(\frac{N}{2}-1)}\end{matrix}\right\}$

a The complex number ϵ in this table denotes $e^{i2\pi/N}$.

Table 6.14 Character table for the group of the wave vectors $k = 0$ and $k = \pi/T$ for achiral nanotubes [135]. This group is isomorphic to the point group D_{2nh}.[a]

D_{2nh}	$\{E\|0\}$	$\cdots$	$2\{C_{2n}^{u}\|vT/2n\}^{s}$	$\cdots$	$\{C_{2n}^{u}\|vT/2n\}^{n}$	$n\{C_2'\|0\}$	$n\{C_2''\|0\}$	$\{I\|0\}$	$\cdots$	$2\{IC_{2n}^{u}\|vT/2n\}^{s}$	$\cdots$	$\{\sigma_h\|0\}$	$n\{\sigma_v'\|0\}$	$n\{\sigma_v''\|T/2\}$
A_{1g}	1	$\cdots$	1	$\cdots$	1	1	1	1	$\cdots$	1	$\cdots$	1	1	1
A_{2g}	1	$\cdots$	1	$\cdots$	1	−1	−1	1	$\cdots$	1	$\cdots$	1	−1	−1
B_{1g}	1	$\cdots$	$(-1)^s$	$\cdots$	−1	1	−1	1	$\cdots$	$(-1)^s$	$\cdots$	−1	1	−1
B_{2g}	1	$\cdots$	$(-1)^s$	$\cdots$	−1	−1	1	1	$\cdots$	$(-1)^s$	$\cdots$	−1	−1	1
⋮	⋮	⋮	⋮	⋮	⋮	⋮	⋮	⋮	⋮	⋮	⋮	⋮	⋮	
$E_{\mu g}$	2	$\cdots$	$2\cos(\mu s\pi/n)$	$\cdots$	$2(-1)^{\mu}$	0	0	2	$\cdots$	$2\cos(\mu s\pi/n)$	$\cdots$	$2(-1)^{\mu}$	0	0
⋮	⋮	⋮	⋮	⋮	⋮	⋮	⋮	⋮	⋮	⋮	⋮	⋮	⋮	⋮
A_{1u}	1	$\cdots$	1	$\cdots$	1	1	1	−1	$\cdots$	−1	$\cdots$	−1	−1	−1
A_{2u}	1	$\cdots$	1	$\cdots$	1	−1	−1	−1	$\cdots$	−1	$\cdots$	−1	1	1
B_{1u}	1	$\cdots$	$(-1)^s$	$\cdots$	−1	1	−1	−1	$\cdots$	$-(-1)^s$	$\cdots$	1	−1	1
B_{2u}	1	$\cdots$	$(-1)^s$	$\cdots$	−1	−1	1	−1	$\cdots$	$-(-1)^s$	$\cdots$	1	1	−1
⋮	⋮	⋮	⋮	⋮	⋮	⋮	⋮	⋮	⋮	⋮	⋮			
$E_{\mu u}$	2	$\cdots$	$2\cos(\mu s\pi/n)$	$\cdots$	$2(-1)^{\mu}$	0	0	−2	$\cdots$	$-2\cos(\mu s\pi/n)$	$\cdots$	$-2(-1)^{\mu}$	0	0
⋮	⋮	⋮	⋮	⋮	⋮	⋮	⋮	⋮	⋮	⋮	⋮	⋮	⋮	⋮

a The values of s and μ span the integer values between 1 and $n - 1$.

Table 6.15 Character table for the group of the wave vectors $0 < k < \pi/T$ for achiral nanotubes [135]. This group is isomorphic to the point group C_{2nv}.

C_{2nv}	$\{E\|0\}$	$2\{C_{2n}^u\|\nu T/2n\}^1$	$\{C_{2n}^u\|\nu T/2n\}^2$	...	$2\{C_{2n}^u\|\nu T/2n\}^{n-1}$	$\{C_{2n}^u\|\nu T/2n\}^n$	$n\{\sigma_\nu'\|0\}$	$n\{\sigma_\nu''\|T/2\}$
A'	1	1	1	...	1	1	1	1
A''	1	1	1	...	1	1	−1	−1
B'	1	−1	1	...	$(-1)^{(n-1)}$	$(-1)^n$	1	−1
B''	1	−1	1	...	$(-1)^{(n-1)}$	$(-1)^n$	−1	1
E_1	2	$2\cos\pi/n$	$2\cos 2\pi/n$	...	$2\cos 2(n-1)\pi/n$	−2	0	0
E_2	2	$2\cos 2\pi/n$	$2\cos 4\pi/n$	...	$2\cos 4(n-1)\pi/n$	2	0	0
⋮	⋮	⋮	⋮	⋮	⋮	⋮	⋮	⋮
$E_{(n-1)}$	2	$2\cos(n-1)\pi/n$	$2\cos 2(n-1)\pi/n$	...	$2\cos(n-1)^2\pi/n$	$2\cos(n-1)\pi$	0	0

Table 6.16 Irreducible representations for the electronic conduction and valence bands of chiral as well as armchair and zigzag achiral nanotubes [135].

		VALENCE		CONDUCTION	
		$k = 0, \pi/T$	$0 < k < \pi/T$	$k = 0, \pi/T$	$0 < k < \pi/T$
CHIRAL	$\mu = 0$	A_1	A	A_2	A
	$0 < \mu < N/2$	E_μ	$\mathbb{E}_{\pm\mu}$	E_μ	$\mathbb{E}_{\pm\mu}$
	$\mu = N/2$	B_1	B	2	B
ARMCHAIR	$\mu = 0$	A_{1g}	A'	A_{2g}	A''
	$0 < \mu < n$	$E_{\mu g}$	E_μ	$E_{\mu u}$	E_μ
	$\mu = n$	B_{1g}	B'	B_{2g}	B''
ZIGZAG	$\mu = 0$	A_{1g}	A'	A_{2u}	A'
	$0 < \mu < n$	$E_{\mu u, \mu g}$ [a]	E_μ	$E_{\mu g, \mu u}$ [a]	E_μ
	$\mu = n$	B_{1g}	B'	B_{2u}	B'

a For zigzag nanotubes, if $\mu < 2n/3$, the valence (conduction) band at $k = 0$ belongs to the $E_{\mu g}$ ($E_{\mu u}$) representation for μ even and to the $E_{\mu u}$ ($E_{\mu g}$) representation for μ odd, while if $\mu > 2n/3$ it is the opposite irreducible representations that apply.

6.4.3
Electrons in Carbon Nanotubes

Having shown the irreducible representations of the wave vector k, it is now possible to obtain the symmetries of the eigenvectors used to describe the electronic and vibrational properties for all the points of the first Brillouin zone. The irreducible representations of the electronic states of chiral nanotubes and achiral nanotubes are summarized in Table 6.16. In general, what defines the symmetry of wavefunctions in the quasi-one-dimensional carbon nanotubes are the number of nodes for the wavefunction phase along the tube circumference. The A modes are totally symmetric, while the E_μ modes exhibit 2μ nodes along the tube circumference, as depicted in Figure 6.8.

6.4.4
Phonons in Carbon Nanotubes

The phonon symmetries also obey the general picture displayed in Figure 6.8. For $k = 0$ phonons in achiral nanotubes (D_{2nh} group), $\Gamma_{\text{vec}} = A_{2u} + E_{1u}$ (z and x, y). The $\Gamma^{\text{a.s.}}$ for zigzag SWNTs is [134, 135]:

$$\Gamma^{\text{a.s.}}_{\text{zigzag}} = A_{1g} + B_{2g} + A_{2u} + B_{1u} + \sum_{j=1}^{n-1} (E_{jg} + E_{ju}) \,, \tag{6.26}$$

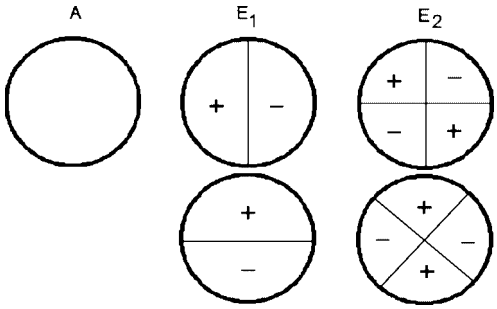

Figure 6.8 Schematics showing the phase change for SWNT wavefunctions with the one-dimensional totally symmetric *A* IR, and the two doubly degenerate E_1 and E_2 IRs.

giving rise to the following irreducible representations for the lattice modes [134, 135]:

$$\Gamma_{\text{zigzag}}^{\text{lat. mode}} = 2A_{1g} + A_{2g} + B_{1g} + 2B_{2g} + A_{1u} + 2A_{2u} + 2B_{1u} + B_{2u} + \sum_{j=1}^{n-1}(3E_{jg} + 3E_{ju}). \tag{6.27}$$

Finding Γ_{vec}, $\Gamma^{\text{a.s.}}$ and $\Gamma^{\text{lat. mode}}$ for armchair and chiral tubes is left as a problem for the reader.

6.4.5 Selection Rules for First-Order Raman Scattering

The optical activity of phonons in a first-order Raman scattering process is easily obtained from the basis functions in the character tables related to the irreducible representations that describe each of the lattice modes. The Raman-active modes are those transforming like symmetric combinations of quadratic functions (xx, yy, zz, xy, yz, zx).

The list of Raman-active modes are given below [134, 135]:

$$\Gamma_{\text{zigzag}}^{\text{Raman}} = 2A_{1g} + 3E_{1g} + 3E_{2g} \rightarrow 8 \text{ modes}, \tag{6.28}$$

$$\Gamma_{\text{armchair}}^{\text{Raman}} = 2A_{1g} + 2E_{1g} + 4E_{2g} \rightarrow 8 \text{ modes}, \tag{6.29}$$

$$\Gamma_{\text{chiral}}^{\text{Raman}} = 3A_1 + 5E_1 + 6E_2 \rightarrow 14 \text{ modes}. \tag{6.30}$$

A more detailed analysis of the Raman-active modes for chiral and achiral nanotubes is provided in [31, 135].

6.4.6
Insights into Selection Rules from Matrix Elements and Zone Folding

To illustrate the usage of the selection rules introduced by the electron–photon and electron–phonon interaction processes, we consider the first-order resonance Raman scattering process in carbon nanotubes. The first-order Raman scattering process involves the following steps: creation of an electron–hole pair, scattering by a phonon, and light emission by an electron–hole recombination process. The Raman signal is greatly enhanced when the electron scatters between VHSs in the valence and conduction band DOS, so that we can consider only the transitions between the two VHSs in the DOS as a first approximation. By utilizing the selection rules introduced above, we come up with the following five cases for allowed first-order resonance Raman scattering processes between the electronic energy VHSs in the valence and conduction bands denoted by $\mathbb{E}_{\mu}^{(v)}$ and $\mathbb{E}_{\mu'}^{(c)}$ [135, 226]:

$$
\begin{aligned}
&\text{(I)} && \mathbb{E}_{\mu}^{(v)} \xrightarrow{\mathrm{Z}} \mathbb{E}_{\mu}^{(c)} \xrightarrow{A} \mathbb{E}_{\mu}^{(c)} \xrightarrow{\mathrm{Z}} \mathbb{E}_{\mu}^{(v)}, \\
&\text{(II)} && \mathbb{E}_{\mu}^{(v)} \xrightarrow{\mathrm{X}} \mathbb{E}_{\mu\pm1}^{(c)} \xrightarrow{A} \mathbb{E}_{\mu\pm1}^{(c)} \xrightarrow{\mathrm{X}} \mathbb{E}_{\mu}^{(v)}, \\
&\text{(III)} && \mathbb{E}_{\mu}^{(v)} \xrightarrow{\mathrm{Z}} \mathbb{E}_{\mu}^{(c)} \xrightarrow{\mathbb{E}_1} \mathbb{E}_{\mu\pm1}^{(c)} \xrightarrow{\mathrm{X}} \mathbb{E}_{\mu}^{(v)}, \\
&\text{(IV)} && \mathbb{E}_{\mu}^{(v)} \xrightarrow{\mathrm{X}} \mathbb{E}_{\mu\pm1}^{(c)} \xrightarrow{\mathbb{E}_1} \mathbb{E}_{\mu}^{(c)} \xrightarrow{\mathrm{Z}} \mathbb{E}_{\mu}^{(v)}, \\
&\text{(V)} && \mathbb{E}_{\mu}^{(v)} \xrightarrow{\mathrm{X}} \mathbb{E}_{\mu\pm1}^{(c)} \xrightarrow{\mathbb{E}_2} \mathbb{E}_{\mu\mp1}^{(c)} \xrightarrow{\mathrm{X}} \mathbb{E}_{\mu}^{(v)},
\end{aligned}
\tag{6.31}
$$

where A, E_1, and E_2 denote the symmetries of the phonon modes at $k = 0$, which are associated with the $\mu = 0, \mu = \pm1$, and $\mu = \pm2$ cutting lines (1D Brillouin zones in 2D k space), respectively. Thus, for a transition to occur between an electron in a state E_{μ_1} and a state E_{μ_2} it is necessary for the phonon which couples the two states to have $E_{\mu_2-\mu_1}$ symmetry. The XZ plane is parallel to the substrate on which the nanotubes lie, the Z axis is directed along the nanotube axis, and the Y axis is directed along the light propagation direction, so that Z and X in Eq. (6.31) stand for the light polarized parallel and perpendicular to the nanotube axis, respectively.

The five processes of Eq. (6.31) result in different polarization configurations for different phonon modes, ZZ and XX for A; ZX and XZ for E_1; and XX for E_2,[28] in perfect agreement with the basis functions predicted by group theory. Also, Eq. (6.31) predicts *different* resonance conditions for *different* phonon modes. While the A and E_1 modes can be observed in resonance for the $\mathbb{E}_{\mu}^{(v)} \rightarrow \mathbb{E}_{\mu}^{(c)}$ and the $\mathbb{E}_{\mu}^{(v)} \rightarrow \mathbb{E}_{\mu\pm1}^{(c)}$ processes, corresponding to E_{ii} and E_{ij} ($j = i \pm 1$) transitions, respectively, the E_2 modes can only be observed in resonance for the $\mathbb{E}_{\mu}^{(v)} \rightarrow \mathbb{E}_{\mu\pm1}^{(c)}$ process. Experimentally observed Raman scattering spectra do follow these predicted polarization configurations and resonance conditions [226–228].

It is also interesting to discuss how equivalent selection rules can be derived considering momentum conservation in the unfolded two-dimensional graphene-

28) ZX corresponds to the linear polarization directions of the incident (Z) and scattered (X) light.

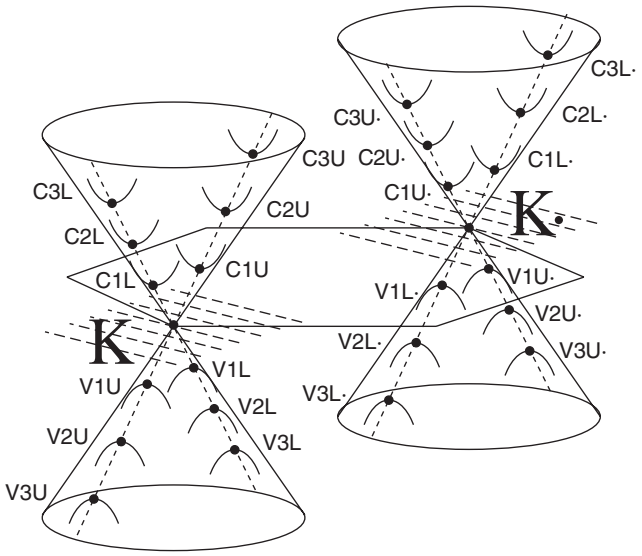

Figure 6.9 The electronic sub-bands for zigzag M-SWNTs in the vicinity of the K and K' points (near the Fermi energy) in the first Brillouin zone. The VHSs are labeled by three symbols: the first denotes the valence or conduction band (C/V), the second denotes the VHS index counted away from the Fermi energy or the cutting line index counted away from the K and K' points, and the third index denotes the lower and upper energy components (L/U) due to the trigonal warping near the $K(K')$ point that distort the cone and splits the energy of the VHSs for metallic SWNTs [229].

sheet, and considering the concepts of cutting lines. This consideration will give insights related to the importance of dimensionality in materials science.

The optical transition in the nanotube is vertical (momentum conserving) within the 1D Brillouin zone, that is, the electronic wave vector along the nanotube axis (along the $\boldsymbol{K}_2$ vector in the unfolded 2D Brillouin zone) does not change. In contrast to the case of the graphene layer, the polarization vector can be either parallel or perpendicular to the nanotube axis for light propagating perpendicular to the substrate on which the nanotubes lie. The dipole selection rules tell us that the optical transition in the nanotube conserves the electronic sub-band index (the cutting line index μ) for light polarized parallel to the nanotube axis. Conservation of both the 1D wave vector and the sub-band index implies conservation of the 2D wave vector in the Brillouin zone of the graphene layer (unfolded Brillouin zone of the nanotube).

As an example, we plot in Figure 6.9 the schematic band diagram of the nanotube in the unfolded 2D Brillouin zone. If the electron starts from the VHS in the valence sub-band V2U (see the solid dot on the sub-band V2U in Figure 6.9), this electron goes to the VHS in the conduction sub-band C2L, and the optical absorption is enhanced substantially because of the extremely high DOS at the VHSs in the valence and conduction sub-bands, V2U and C2L. If an electron in the valence sub-band V2U in Figure 6.9 absorbs a photon polarized perpendicular to the

nanotube axis (i. e., polarized along the $\boldsymbol{K}_1$ vector), it can scatter to one of the two conduction sub-bands, either C1L or C3L, depending on the photon frequency and on the interband transition energies $E_{2,1}$ and $E_{2,3}$. This implies a different set of VHSs in the JDOS for perpendicular polarization, $E_{\mu,\mu\pm1}$, and these energies are located between the VHSs in the JDOS for parallel polarization, $E_{\mu\mu}$.

While the optical transition is vertical for the light polarized parallel to the nanotube axis, it involves a wave vector change of $\pm\boldsymbol{K}_1$ (the distance between two adjacent cutting lines) for the perpendicular polarization. This wave vector change can be understood by considering an unrolled nanotube, as shown in Figure 6.10. When the nanotube is unrolled into the graphene layer, the light polarized parallel to the nanotube axis transforms into light polarized parallel to the graphene layer, as shown in Figure 6.10a. This results in a vertical interband optical transition in the unfolded 2D Brillouin zone, which is equivalent to the optical transition within the same sub-band μ in the folded 1D Brillouin zone of the nanotube, as is predicted by the dipole selection rules.

However, perpendicular polarization in nanotubes becomes transformed into the in-plane and out-of-plane polarizations in the unfolded graphene layer, periodically modulated along the direction of the $\boldsymbol{C}_h$ (or $\boldsymbol{K}_1$) vector with the period $|\boldsymbol{C}_h| = \pi d_t$ (nanotube circumference), as shown in Figure 6.10b [110]. The optical transitions induced by the out-of-plane polarization are expected to be much weaker compared to those induced by the in-plane polarization and are usually ignored, because of the much stronger in-plane interaction in the graphene layer [220]. This implies that the light polarization in the unrolled nanotube shown in Figure 6.10b can be considered, as a first approximation, to be parallel to the graphene layer, with an additional phase factor describing oscillations of the in-plane polarization component, arising from the rotation of the polarization vector. The phase factor is given by $\cos(\boldsymbol{k}\cdot\boldsymbol{r})$ where the wave vector $\boldsymbol{k}$ has the direction of $\boldsymbol{K}_1$ and a magnitude of $2\pi/(\pi d_t) = 2/d_t$, that is, $\boldsymbol{k} = \boldsymbol{K}_1$. By assuming wave vector conservation in the unfolded 2D Brillouin zone for the optical transition process, we come up with the selection rules $\boldsymbol{k}_c = \boldsymbol{k}_v \pm \boldsymbol{K}_1$ for light absorption and $\boldsymbol{k}_v = \boldsymbol{k}_c \pm \boldsymbol{K}_1$ for light emission, which correspond to an electronic transition to the adjacent cutting line in the unfolded 2D Brillouin zone, or the electronic transition to the adjacent sub-band in the 1D Brillouin zone of the nanotube. It is interesting to note that the photon wave vector $\pm\boldsymbol{K}_1$ in the unrolled graphene layer is much larger in magnitude than the photon wave vector κ in free space, $K_1 = 2/d_t \gg \kappa = 2\pi/\lambda$, because the nanotube diameter d_t is much smaller than the optical wave length λ. Therefore, an

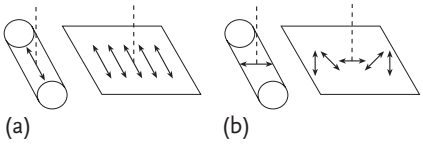

Figure 6.10 Light polarization (a) parallel and (b) perpendicular to the nanotube axis, shown for both a rolled-up SWNT, and a SWNT unrolled into the graphene layer. The arrows show the light polarization vector, and the dashed lines show the light propagation direction [110].

optical photon in the unrolled graphene layer can be considered as an X-ray photon with respect to spatial considerations, yet the photon energy does not change when the nanotube is unrolled into the graphene layer. Such a "pseudo X-ray" photon is a source of breaking the optical selection rules in the case of perpendicular polarization.

The selection rules for the scattering of electrons by phonons can also be obtained by momentum conservation in 2D graphite. Two cutting lines belonging to the irreducible representations E_μ and $E_{\mu'}$ are separated from each other in the 2D Brillouin zone by $\boldsymbol{k} - \boldsymbol{k}' = (\mu - \mu')2\pi/d_t$, and this is the momentum that the phonon should transfer as a result of the optical transition. As explained in Section 6.4.4, the symmetry of the phonon with such a momentum can be obtained by rolling up the 2D graphene layer and this will yield a phonon with $E_{\mu-\mu'}$ symmetry.

Problems

[6-1] Check the applicability of Eq. (6.2) for group $P(3)$ and for the group of symmetry operations of an equilateral triangle.

[6-2] Propose a unitary matrix and apply the unitary transformation to Γ_R in Eq. (6.7).

[6-3] Show that the traces for the IRs in Eq. (6.5) actually give the characters for the character table in Table 6.2. Show that the Wonderful Orthogonality Theorem works for all possible combinations of IRs. Show that a similar theorem can be made for orthogonality between classes.

[6-4] Consider a CH_4 molecule which has T_d symmetry. Obtain from some textbook the character table for T_d symmetry. Which irreducible representations correspond to the vector (x, y and z)? Show the matrix for a C_3 rotation of this molecule.

[6-5] Which irreducible representations of the T_d group correspond to rotations around the x, y and z axes? Explain that the results do not depend on how you select the axes.

[6-6] Obtain the atom site representation for a CH_4 molecule and decompose your atom site representations into a set of irreducible representations.

[6-7] Calculate the reducible representation for the molecular vibrations for the CH_4 molecule and decompose the reducible representation into irreducible representations. How many vibrational modes are there for a CH_4 molecule?

[6-8] Obtain the symmetries of the Raman and IR-active phonon modes of a CH_4 molecule. In the case of a CH_4 molecule, show that there is no inversion symmetry both by plotting a model of the CH_4 molecule and by showing its atomic coordinates.

[6-9] Now let us consider the single atomic layer of graphite which we call graphene. Consider the character table of the point group for the hexagonal unit cell of monolayer graphene. Obtain the atom site representation of the two carbon atoms of graphene.

[6-10] Obtain the symmetry of the vibrations of graphene at the zone center of the Brillouin zone for graphene.

[6-11] Obtain the symmetry of the tight-binding orbitals of graphene at the zone center of the Brillouin zone.

[6-12] Show that an optical transition from one $2p$ carbon atomic orbital to another $2p$ carbon atomic orbital within the same carbon atom is not allowed. On the other hand, the optical transition from π to π^* energy bands is allowed. Explain what kind of matrix element contributes to such an optically allowed transition? Expand the tight-binding wavefunctions for the optical transition matrix.

[6-13] In the case of graphene, optical transitions occur around the hexagonal corners of the Brillouin zone (K and K' points). When we consider a large unit cell, the K point can be folded into the Γ point (zone center). Plot the extended unit cell and the folded Brillouin zone. What is the point group for the extended unit cell?

[6-14] We can consider a C_2 rotation around the axis at the center of the C–C atomic bond in the direction perpendicular to the bond. However, this rotation is not included in the operations for the hexagonal unit cell of graphene. On the other hand, when we consider the rhombic unit cell of graphene, we can include the C_2 rotation. Discuss the difference in the results of a symmetry description for the two different shapes of the unit cell of graphene.

[6-15] Consider the point group of double layer graphene, in which the two layers have AB stacking. Obtain the irreducible representations for the atom sites and vibrations of bilayer graphene.

[6-16] In the case of double layer graphene with AB stacking, the interlayer interaction can be treated as a perturbation to the unperturbed two graphene layers. What is the irreducible representation describing the interlayer interaction?

[6-17] For double layer graphene, we expect four energy bands derived from the π and π^* bands. Obtain the irreducible representations for the four electronic energy bands at the zone center. Here and in the next graphene related problems, we always consider the AB Bernal stacking.

[6-18] For double layer graphene, show by group theory that the four π bands at the K point consist of one doubly degenerate energy state and two nondegenerate energy states. Discuss the optical selection rules of monolayer graphene and bilayer graphene near the K point.

[6-19] Discuss the Raman selection rules for the vibrations occurring in monolayer graphene and in bilayer graphene.

[6-20] Discuss the symmetry for trilayer graphene and obtain the symmetries of its Raman-active modes. Obtain the optical selection rules for triple layer graphene.

[6-21] Discuss the symmetry for four layer graphene and obtain the symmetries of its Raman-active modes. Obtain the optical selection rules for four layer graphene.

[6-22] When we consider three-dimensional graphite with AB layer stacking, show the point group of the graphite unit cell and discuss the IR and Raman-active modes for graphite.

[6-23] Discuss the symmetry of a unit cell for a graphene ribbon with zigzag edges or one with armchair edges. What is the difference in the symmetry of these unit cells relative to the symmetry of a unit cell for monolayer graphene?

[6-24] The C_{60} molecule has I_h symmetry. Find the atom site irreducible representations and symmetries of the vibrational modes for the C_{60} molecule. How many Raman-active modes are there for the C_{60} molecule and what are their symmetries?

[6-25] Obtain Eqs. (6.22), (6.23) and (6.24).

[6-26] Demonstrate how Eqs. (6.26) and (6.27) are obtained.

[6-27] Consider (n, n) armchair single-wall carbon nanotubes. Obtain Γ^{vec}, $\Gamma^{\text{a.s.}}$, $\Gamma_{\text{lat. mode}}$ and discuss their Raman-active modes.

[6-28] Consider (n, m) chiral single wall carbon nanotubes ($n \neq m$). Obtain Γ^{vec}, $\Gamma^{\text{a.s.}}$, $\Gamma_{\text{lat. mode}}$ and discuss their Raman-active modes.

Part Two Detailed Analysis of Raman Spectroscopy in Graphene Related Systems